Vesicular Monoamine Transporters: Structure-Function, Pharmacology, and Medicinal Chemistry

Kandatege Wimalasena
Department of Chemistry, Wichita State University, Wichita, KS 67260, Phone; (316) 978-7386

Kandatege Wimalasena: kandatege.wimalasena@wichita.edu

Abstract

Vesicular monoamine transporters (VMAT) are responsible for the uptake of cytosolic monoamines into synaptic vesicles in monoaminergic neurons. Two closely related VMATs with distinct pharmacological properties and tissue distributions have been characterized. VMAT1 is preferentially expressed in neuroendocrine cells and VMAT2 is primarily expressed in the CNS. The neurotoxicity and addictive properties of various psychostimulants have been attributed, at least partly, to their interference with VMAT2 functions. The quantitative assessment of the VMAT2 density by PET scanning has been clinically useful for early diagnosis and monitoring of the progression of Parkinson's and Alzheimer's diseases and drug addiction. The classical VMAT2 inhibitor tetrabenazine has long been used for the treatment of chorea associated with Huntington's disease in UK, Canada and Australia and recently approved in the US. The VMAT2 imaging may also be useful for exploiting the onset of diabetes mellitus, since VMAT2 is also expressed in the β-cells of the pancreas. VMAT1 gene SLC18A1 is a locus with strong evidence of linkage with schizophrenia and thus, the polymorphic forms of the VMAT1 gene may confer susceptibility to schizophrenia. This review summarizes the current understanding of the structure-function relationships of VMAT2, and the role of VMAT2 on addiction and psychostimulant induced neurotoxicity, and the therapeutic and diagnostic applications of specific VMAT2 ligands. The evidence for the linkage of VMAT1 gene with schizophrenia and bipolar disorder I are also discussed.

Keywords

Vesicular Monoamine Transporter 1 (VMAT1); Vesicular monoamine transporter 2 (VMAT2); Psychostimulant abuse; Catecholamine metabolism; Synaptic vesicles; Oxidative stress; Parkinson's disease

1. Introduction

Monoamine neurotransmission constitutes several critical steps in the synaptic area of the neuron including (i) biosynthesis of transmitters from precursors in the cytosol and active accumulation into synaptic vesicles through a proton gradient driven uptake system; (ii) continued biosynthetic transformations within the synaptic vesicles depending on the nature of the transmitter followed by exocytotic release from the synaptic vesicles into the synaptic cleft in response to physiological stimuli; (iii) interaction of the transmitter with their target receptor or protein on the postsynaptic membrane thereby mediating signal transduction; (iv) dissociation from the receptor or protein followed by re-uptake into the presynaptic terminal or surrounding glia cells through Na^+ and Cl^- driven plasma membrane transporters or inactivation by specific monoamine metabolizing enzymes. Thus, efficient re-uptake of the transmitter from the synaptic cleft through plasma membrane monoamine transporters followed by re-accumulation into synaptic vesicles through the vesicular monoamine

transporters (VMATs) constitute crucial steps of monoamine neurotransmission (general reviews)[1–3].

Numerous studies indicate that VMATs play a critical role not only in sorting, storing, and releasing of neurotransmitters, but also in fine-tuning the neuronal and endocrine informational output (reviews)[4–7]. In addition, neuropharmacological and neurotoxic effects of a large number of illicit drugs and neurotoxins are closely associated with their interference with the physiological functions of VMATs. For example, increasing evidence suggests that amphetamine-related illicit drugs exert their effects by increasing the non-exocytotic release of dopamine (DA) in some regions of the brain through direct interaction with VMATs (reviews)[8–10]. Similarly, the neurotoxicity of the Parkinson's disease causing toxin, 1-methyl-4-phenylpyridinium (MPP^+), is believed to be at least partly due to its ability to interfere with the vesicular uptake and storage of DA through VMAT in DA neurons[11–13]. Therefore, the malfunctions of VMAT could lead to the perturbation of catecholamine metabolism and increase of cytosolic catecholamine levels leading to increased oxidative stress and eventual degeneration of the catecholaminergic nervous system (review)[14].

2. Vesicular Monoamine Transporters

Adrenergic chromaffin granules and synaptic vesicles maintain a high concentration (up to 0.5 M) of monoamines. VMATs are responsible for the efficient uptake of cytosolic monoamines into the storage vesicles[4–7]. The active transport of cytosolic monoamines into storage vesicles, against a high concentration gradient, is driven by a transmembrane pH and electrochemical gradient generated by the vesicular H^+-ATPase in the granule membrane. Two closely related vesicular monoamine transporters, VMAT1[15–16] and VMAT2[15,17] have been cloned, expressed and characterized. In humans, VMAT1 is preferentially expressed in large dense core vesicles of various neuroendocrine cells, including chromaffin and enterochromaffin cells[18,19]. VMAT2 is primarily expressed in multiple monoaminergic cells in the brain, sympathetic nervous system, mast cells, and histamine containing cells in the gut[19–20]. VMAT1 and VMAT2 are co-expressed in chromaffin cells of the adrenal medulla. Interestingly, the organ distribution of the two transporters appears to be species dependent[21]. While rat adrenal medulla exclusively express VMAT1, VMAT2 is the major transporter in chromaffin granules of the bovine adrenal medulla[7,22–23]. The physiological significance of these differences is not clearly understood.

VMAT1 and VMAT2 are acidic glycoproteins with an apparent molecular weight of 70 kDa[15–17]. Although derived from two different genes, they show high sequence homology. A third member of the family, the vesicular acetylcholine transporter (VAChT) also shows significant sequence homology to both VMAT proteins (reviews)[24–25]. While the crystallographic structures are not resolved, the sequence analyses of these and related proteins suggest that they are transmembrane proteins with 12 transmembrane domains similar to plasma membrane monoamine transporters (Fig. 1 [26]). The absence of a cleavable signal sequence in VMAT2 expressed in CV-1 cells indicates that both C- and N-terminals of these transporters are located in the cytosolic phase of the vesicle[17]. According to the hydropathy models, putative glycosylation sites (three or four) are located in the vesicular matrix on a loop between transmembrane domain (TMD) I and II (Fig. 1). The same overall model is predicted to be common to VMAT-1 and VMAT-2 from all origins, as well as the acetylcholine transporter (VAChT). The most variable regions of these proteins are located near the N- and C- terminal and in the large glycosylated loop between transmembrane domains (TMD) I and II (Fig. 1). For instance, the homology between bovine VMAT-1 and VMAT-2 in the glycosylated loop is only 22%(residues 38–131).

3. Biochemical and Kinetic Characteristics of VMAT

3.1 Adrenal Chromaffin Granule VMAT

The current understanding of the bioenergetics of VMAT-mediated monoamine transport has been largely derived from the results of extensive biochemical and biophysical studies carried out with bovine adrenal chromaffin granules[1-6, 27]. The ATP dependent, reserpine (RES) sensitive catecholamine uptake into bovine chromaffin granules through VMAT was initially demonstrated by Kirshner[28]. Since then numerous biophysical studies have confirmed that the transport of monoamine into the storage vesicles against a large concentration gradient ($>10^5$) is driven by a combination of transmembrane proton and electrochemical gradients generated by vesicular H^+-ATPase. The inward transport of cytosolic amine is coupled with the efflux of two protons from the granule matrix per amine molecule[24,29-31]. The efflux of the first proton from the granule matrix is proposed to generate a transporter conformation with a high affinity amine binding site in the cytosolic phase. The efflux of the second proton is coupled with a second large conformational change leading to the movement of the amine from the cytosolic phase to the matrix phase with the concomitant reduction of the amine binding affinity[24]. The interaction of the classical inhibitor RES with chromaffin granule VMAT is also modulated by the transmembrane pH gradient[30]. The transmembrane pH gradient was shown to increase the rate of RES binding to chromaffin granule VMAT. In addition, VMAT bound RES could also be effectively replaced with micromolar concentrations of the substrate norepinephrine (NE). However, the pH gradient or NE has no effect on the tetrabenazine (TBZ), dihydrotetrabenazine (DTBZOH), or ketanserin (KET) bindings. These findings have led to a working model in which RES and the substrate bind to a single site in the pH gradient modulated conformation of the transporter, whereas TBZ and DTBZOH bind to a different site or different conformation of the transporter. However recent structure-activity studies indicate that the RES and TBZ binding sites of the VMAT may overlap at least partially(*see* below).

The initial rate kinetics of the interaction of physiological substrates and various pharmacological agents with VMAT has also been studied using intact bovine chromaffin granules or granule ghosts. The apparent K_m and V_{max} parameters determined for 5-hydroxytryptamine [serotonin; 5HT (**1**)], DA (**2**), NE (**3**), and epinephrine [E (**4**)] using resealed chromaffin granule ghosts are shown in Table I. Comparison of the V_{max}/K_m parameters show that the uptake efficiencies of these amines are in the order of 5HT> DA > E > NE. Similarly, the kinetics of the interactions of TBZ (**5**), RES (**6**), KET (**7**), and DTBZOH (**8**) with the bovine chromaffin granule have also been studied in detail. The experimentally determined dissociation constants (K_ds) for these inhibitors are in low nM range suggesting that they all are very potent inhibitors for the monoamine uptake system in chromaffin granules (Table I).

3.2 Brain Synaptic Vesicle VMAT

The catecholamine uptake characteristics of synaptic vesicles isolated from whole brain as well as various brain regions have also been reported[37]. While many primary characteristics of the brain's synaptic vesicles are similar to chromaffin granules, there are some important differences that are worth mentioning; (a) the affinity of catecholamines for the brain catecholamine uptake system is significantly higher than that of the chromaffin granules (Tables I & II and references therein); (b) although, the catecholamine uptake into chromaffin granules is dependent only on the magnitude of the transmembrane proton and electrochemical gradients according to the chemiosmotic model, catecholamine uptake into synaptic vesicles appear to be also dependent on the cytoplasmic concentration of the transmitters[38], the transporter density in the vesicle membrane[39], and the composition of the extra vesicular media[39-40]; (c) while the catecholamine content in bovine adrenal

chromaffin granules is estimated to be 0.5 M, there is no evidence for such high concentrations in brain synaptic vesicles.

The origins of the above differences are not clear at present. However, the heterogeneity of brain vesicle preparations must be taken into account in detailed interpretation of the kinetic data. On the other hand, previous studies have shown that the transient kinetics of the DA accumulation and NE production in resealed bovine chromaffin granule ghosts were inconsistent with a normal sequential uptake followed by the conversion process. However, they were consistent with a mechanism in which DA is efficiently channeled from the VMAT to membranous dopamine β-monooxygenase (DβM) for hydroxylation, prior to the release into the bulk medium of the ghost interior [33]. Therefore, K_m parameters determined under the steady state conditions for DA using resealed granule ghosts or intact granules will not directly reflect the affinity to VMAT. Since the K_m of DA for DβM is in the low mM range, the experimentally determined K_m parameters from the steady-state uptake data must be significantly higher for chromaffin granules and granule ghosts in comparison to brain DA or 5HT synaptic vesicles as well as all the heterologous VMAT expression systems (*see* below and Table 1 & II). This complexity could also be associated with the noradrenergic and adrenergic synaptic vesicles. On the other hand, the K_i parameters of VMAT inhibitors (non-substrates) are devoid of this complexity and directly reflect the true affinity for VMAT. Therefore, while the K_m values determined for VMAT substrates using various systems could vary greatly, the K_i parameters are largely independent of the system used and could be compared directly (for example see Table I & II).

3.2 Heterologous Expression Systems

CV-1 cells expressing VMAT accumulate [^{3}H]5HT although they do not contain storage vesicles[17]. [^{3}H]5HT accumulation was ATP dependent, inhibited by H$^+$-ATPase inhibitors and increased by the digitonin permeabilization of the plasma membrane, suggesting [^{3}H]5HT accumulation in acidic intracellular compartments of CV-1 cells. Therefore, degitonine permeabilized CV-1 cells expressing VMAT1 or VMAT2 have been used as a model to screen the relative substrate and inhibitor affinities for the two transporters. Studies using this model have shown that while 5HT has a similar affinity for both transporters, DA, NE, and E have a 3-fold higher affinity for VMAT2[20]. Interestingly, histamine (**9**) has a 30-fold higher affinity for VMAT2 in comparison to VMAT1. Both RES and KET are slightly more potent inhibitors of VMAT2-mediated transport [^{3}H]5HT than that of VMAT1, whereas TBZ is a relatively specific inhibitor of VMAT2 (Table II). Phenylethylamine (**10**), amphetamine [AMPH (**11** & **12**)], methylenedioxy methamphetamine [METH (**13**)] and N-methyl-4-phenylpyridinium (**15**) are all more potent inhibitors of VMAT2 mediated [^{3}H]5HT transport than that of VMAT1, whereas fenfluramine (**14**) is a more potent inhibitor of VMAT1-mediated [^{3}H]5HT transport than that of VMAT2 (Table II). Comparative kinetic studies with CHO cells expressing bovine chromaffin granule VMAT (bVMAT) show substrate specificities and affinities similar to that of VMAT2 (Table II)[42]. In addition, TBZ is also a high affinity inhibitor for bVMAT. These findings further confirm that the major monoamine uptake system in bovine chromaffin granules is similar to VMAT2 in contrast to rat chromaffin granules. Therefore, significance of the species specific expression of two distinct forms of monoamine transporters is not clear at present. In addition, as mentioned above, while the K_i or K_m parameters determined using heterologus VMAT expression systems may provide a measure of the affinity of various substrates and inhibitors for VMAT, they may not directly reflect the physiological affinities of these agents due to the complex interactions of VMAT with other synaptic vesicle proteins (see above).

4. Structure-function Relationship Studies

Mutagenesis

Several laboratories have used heterologous expression systems to gain insight into the structure-function relationships of VMAT at the molecular level. In a series of original studies, Shirvan *et. al.*[43] have shown that the mutation of the His419 (His414 in hVMAT2) in the cytoplasmic domain between TMD X and XI of rat VMAT1 (r-VMAT1) to either Arg or Cys completely abolishes 5HT and DA accumulation and also inhibits the pH gradient dependent acceleration of binding of RES. These observations have been used to conclude that His419 plays a role in energy coupling to the amine transport probably through assisting the first proton dependent conformational change of the transporter [RES was proposed to interact with this conformation (see above)]. The replacement of Asp431 (Asp426 in hVMAT2) in TMD XI with either Glu or Ser inhibits 5HT transport without affecting the rate of RES binding[44]. Therefore, the Asp431 residue is necessary for the completion of the substrate transport cycle i.e. the proposed second conformational change in the above model. On the other hand, replacement of Asp404 (Asp399 in hVMAT2) in TMD X with either Ser or Cys inhibits 5HT transport and affects the RES binding properties of r-VMAT1 as well[44]. However, 5HT transport or the RES and TBZ binding is not significantly altered by the replacement of Asp404 with Glu suggesting a critical role of the carboxyl moiety at position 404 in r-VMAT1 catalytic function.

Analysis of the VMAT sequences show that four aspartic acid residues in the middle region of TMD I, VI, X and XI and one Lys residue in TMD II are highly conserved among all members (Figure 1), implicating their critical role in transporter structure/activity. Merickel *et al.* have systematically examined the role of these residues in the structure-activity of rVMAT2[45]. The replacement of conserved Lys 139 of TMD-II (Lys 138 of hVMAT2) with Ala (K139A), Asp 400 (Asp 399 of hMAT2) of TMD-X with Asn (D400N) or Asp 427 (Asp 426 of hMAT2) in TMD-XI with Asn (D427N) eliminate the transport activity despite the normal levels of the expression of mutated proteins in agreement with the above rVMAT1 studies of Steiner-Mordoch *et al.*[44]. However, the replacement of Asp 263 (Asp 262 of hVMAT2) of TMD-VI with Asn (D263N) had no effect on the transport activity. Interestingly, the double replacement of Lys 139 and Asp 427 (K139A/D427N) showed substantial transporter activity. Based on these observations together with literature evidence from the studies of lactose permease[45], the authors concluded that Lys 139 and Asp 427 may make an ion pair and that TMD-II and TMD-XI are close to each other in the native form of the transporter. However, the apparent reduced affinity of the double mutant K139A/D427N for 5HT and reduced ability of 5HT to inhibit RES binding suggest that although not required for activity, the ion pair may promote high affinity interaction with the substrates and inhibitors. In addition, a double mutant in which the polarity of these charged residues was reversed (K139D/D427K) showed no active transport, but displayed normal RES binding that remained coupled to the proton gradient. However, 5HT failed to inhibit RES binding of the mutated protein significantly. A similar effect has also been observed with Asp 33 (Asp 33 of hMAT2) in TMD-I (D33N). Therefore, while these residues may play a role in the recognition of the substrate, they may not be essential for the flux of the first proton and subsequent conformational change of the transporter.

Studies with chimeric constructs of rVMAT1 and rVMAT2 indicate that two domains, one from TMD-V to the beginning of TMD-VIII and the other from the end of TMD-IX to TMD-XII, are required for the characteristic high affinity for 5HT and histamine as well as the sensitivity to TBZ of VMAT2[46]. However, the region of VMAT2 from TMD-III through TMD-IV contributes to the high affinity of 5HT but not histamine or TBZ affinity. Thus, differences between 5HT recognition and the recognition of both histamine and TBZ may account for the observed differences in their interaction with the transport protein. Site-

directed mutagenesis studies further showed that Ala 315 (loop between TMD VI and VII; Ala 314 of hVMAT2) of VMAT2 is required for TBZ sensitivity, and this interaction occurs independently of the interaction with residues in TMD IX-XII. The ability to recognize histamine as a substrate depends on Pro 237 (Pro 236 of hVMAT2) of TMD-V, and the contribution of TMD IX-XII to histamine recognition appears to involve a common mechanism. In contrast, the replacement of many residues in TMD V-VIII of VMAT2 with equivalent residues from VMAT1 improves the recognition of both 5HT and tryptamine and these effects are dominant over mutations in TMD IX-XII. The replacement of the individual residues in TMD IX through XII of VMAT2 by the corresponding residues of VMAT1 indicates that Tyr 434 (Tyr 433 of hVMAT2) and Asp 461 (Asp 460 of hVMAT2) are important for the high affinity of TBZ, histamine, and 5HT towards VMAT2[46]. These results indicate that different ligands interact through distinct mechanisms with the VMATs and that the recognition of each ligand involves multiple, independent three dimensional interactions with the multiple domains of the transporter[47].

To determine the role of the 10 cysteine residues in hVMAT2 function[48], hVMAT2 constructs with reduced number of cysteines have been engineered and characterized. The biochemical studies of the engineered proteins show that Cys 430 in TMD XI is essential for the recognition and binding of TBZ. This finding is in good agreement with the above mutagenesis studies where the involvement of the residues in TMD X-XII in TBZ binding has been proposed. In addition, using a recombinant VMAT2 construct with a thrombin cleavage site between TMD VI and VII demonstrated that Cys 117 in the loop between TMD I and II and Cys 324 in the loop between TMD VII and VIII form a disulfide bond in hVMAT2 which contributes to the structural integrity and efficient monoamine transport[49]. These findings further suggest that these two loops are in close proximity of the native protein (note that the Cys residues of hVMAT2 are mislabeled in the references [48] and [49] consistently by +9 residues; for example Cys 117 and 324 were labeled as Cys 126 and 333).

Photoaffinity Labeling

The substrate and inhibitor binding sites of VMAT have also been exploited using affinity labeling techniques. The affinity photolabel [^{125}I]-7-azido-8-iodoketanserin (**16**) which binds to the same site as RES, is shown to label a site in bVMAT2 of intact bovine chromaffin granule membranes[50]. Degradative analysis of the labeled protein identified a site located between the residues 2–55 as the photo-labeling site. Parallel studies using purified rVMAT2 (expressed in Sf9 cells using a baculovirus expression system) showed the labeling of Lys 20 by [^{125}I]-7-azido-8-iodoketanserin[51]. These findings strongly suggest that the N-terminal residues of VMAT2 play an important role in the recognition and binding of classical inhibitors KET, RES and, possibly, TBZ. The TBZ derivative [^{125}I] 2-N-[(3′-iodo-4′-azido-phenyl) propionyl] tetrabenazine [Table VII (**17**)] also labeled a segment of rVMAT2 between Gly 408 and Cys 431 in TMD X and XI[51]. This evidence has been used to suggest that the TMD I and X/XI are close to each other in native VMAT2 which is in good agreement with the mutagenesis studies where TMD II and TMD XI were proposed to be in close proximity. In a recent study, the novel photo-affinity label [^{125}I]iodoaminoflisopolol [Scheme 1 (**18**)] (an apparent substrate for rVMAT2 with K_m and V_{max} of 122 μM and 292 nmols/mg.min) has been used to identify the substrate binding site of rVMAT2 using a heterologous Sf9 cell expression system[52]. These studies have provided further evidence to support that the substrate binding site of VMAT2 is located in the C-terminal half of the VMAT2 molecule whereas TBZ and KET interact with the N-terminal half [52].

Substrate/Inhibitors and Structure-Function

In addition to mutagenesis, chimeric and labeling studies of novel inhibitors and substrates have also been used to map the steric and electronic constraints of the active sites of VMATs. The phenyl ethylamine analog, 3-amino-2-phenylpropene [APP (**19**)] and its derivatives are competitive inhibitors for the bovine chromaffin granule VMAT2 (Table III)[53]. While the 4′ or 3′-OH groups of the aromatic ring of APP (**20** & **21**) enhance the inhibition potency, -Me (**28**) or -OMe (**22** & **23**) groups in these positions reduce the inhibition potency suggesting an important role of the ring hydroxyl groups of the inhibitor in the interaction with the transporter (Table III). However, large halogen substitution on the 4′-position of the aromatic ring (**24–27**) also causes an increase of the inhibition potency which is parallel to the electron donor ability of the halogen. Although this behavior is inconsistent with the proposed critical role of the polar 4′-ring hydroxyl groups of the substrates, the authors argued that electronic effects of ring halogens on the phenylpropene moiety of the inhibitors may contribute to these effects. Substituents on the $-NH_2$ (**29** – **31**), as well as on the 3-position of the alkyl chain (**33**) reduce the inhibition potency. Based on the structure-activity relationship analyses of APP inhibitors and VMAT substrates, tyramine and the neurotoxin, 1-methyl-4-phenylpyridinium, the conformationally restricted mobility of the side chain of APP, in comparison to the regular phenylethylamine substrate, have been proposed to play a critical role in the inhibition of bVMAT2 by APP derivatives.

The structural rigidity and the good substrate activity of MPP[+11−12, 54] (**15**), in comparison to physiological phenylethylamine substrates, make it an attractive candidate for structure-activity relationship studies of VMAT[55]. Based on this rational, a number of MPTP and MPP[+] derivatives have been synthesized and characterized as novel substrates/inhibitors for bVMAT2 (Table IV). These studies have shown that 3′-OHMPP[+] (**39**) is one of the best known substrates for bVMAT2. It also effectively inhibits the DA uptake into resealed granule ghosts. Based on the magnitudes of apparent K_i parameters determined for DA uptake inhibition, 3′-OH MPP[+] interacts about ten times better than DA and about thirty five times better than the parent compound, MPP[+] with bVMAT2. However, 4′-OHMPP[+] (**40**) was a weak substrate and an inhibitor of bVMAT2 in sharp contrast to the effects of 4′-OH substitution in physiological phenylethylamine substrates and APP inhibitors above. Strikingly, 4′-bulky halogen substitution (**44**) also increased the inhibition potency of the MPP[+] derivatives similar to APP derivatives. However, these derivatives were not substrates for the transporter suggesting that the transport through bVMAT2 requires more stringent structural requirements than the inhibition. Furthermore, the relative orientation of the 3′-OH and the ring nitrogen in 3′-OH MPP[+] may be optimal for the bVMAT2 substrate activity. Interestingly, MPTP derivatives are also good inhibitors of bVMAT2 [Table IV (**51–58**)] and the structure activity relationships of these follow a trend similar to that of MPP[+].

A series of probes that mimic the structural features of both APP (inhibitor) and MPP[+] (substrate) have been used to further characterize the interaction of substrate and inhibitors with bVMAT2 (Table V). None of the MPP[+]-APP conjugates were substrates for the VMAT, but they were better inhibitors than either the corresponding APP or MPP[+] derivatives, suggesting that both entities of the conjugate positively contribute to the interaction with the transporter. Crystallographic structures of these derivatives (structure of **64** is shown in Fig. 2) show that they all possess a well-defined "L" shape architecture and both APP and MPP[+] portions could interact with the transporter as two separate entities leading to higher inhibition potencies in comparison to the parent derivatives. The modeling studies show that the MPP[+]-APP conjugates structurally resemble RES and TBZ (Figures 3A & B). Overlay of the optimized structures of **65** and TBZ shows that the two molecules are similar with respect to steric constraints and positioning of the 4′- and 3′-phenyl ring oxygen substituents. However, the ring nitrogens could not be fully overlaid keeping the above constraints intact indicating that the nitrogens of bVMAT2 bound **65** and TBZ may

not occupy the same positions of the active site. Similar modeling with RES shows that the non-aromatic nitrogen of RES and the pyridine nitrogen of **65** superimpose well (Fig. 3), suggesting that they could occupy similar positions in the binding site. These proposals are consistent with the finding that the replacement of the pyridine ring of the MPP$^+$ portion of **59** with nonaromatic piperidine (**61**) or piperazine (**63**) increases the inhibition potency significantly (Table V). Thus, the high affinity of TBZ ($K_i \sim 4$ nM; Table I & VII) in comparison to the MPP$^+$-APP conjugates could be due to the optimal positioning of the nitrogen and the carbonyl oxygen (or -OH of DTBZOH) in the binding site which are not present in MPP$^+$-APP conjugates or RES. The large trimethoxyphenyl tail of RES could not be mimicked by TBZ or any of the above MPP$^+$-APP conjugate inhibitors. Thus, since the carbonyl oxygen is not present and nitrogens of RES may not contribute towards optimal binding, its extended hydrophobic tail must provide significant non-specific contribution towards its high binding affinity, especially since the binding site of the transporter is shown to be highly hydrophobic. This proposals are in good agreement with the previous reports that the trimethoxyphenyl acetate-cleaved RES derivative, reserpic acid, is at least a 2000-fold weaker inhibitor than RES [K_i's of RES and reserpic acid are ~18 nM (Table I) and ~10 μM[56] respectively]. Since the above conjugates may not have optimal positioning of the nitrogen as well as lacking an extended hydrophobic tail, they are substantially weaker inhibitors for VMAT in comparison to TBZ and RES, but comparable to reserpic acid. The excellent substrate activity of 3′-OH MPP$^+$ in comparison to the weak activity of 4′-OH MPP$^+$ suggests that the relative positioning of 3′-OH with respect to pyridine nitrogen in MPP$^+$ derivatives is optimal for the VMAT substrate activity. Thus, similar inhibition potencies observed for the MPP$^+$-APP conjugates with respect to 3′- and 4′-OH further indicate that the mode of interaction of these as well as RES and TBZ inhibitors with the transporter could be distinct from that of regular substrates.

The lipophilic alkaloid lobeline [Table VI (**68**)] which is a known nicotinic receptor ligand is also an inhibitor of DAT and VMAT2[57]. Lobeline inhibits [^{3}H]DTBZOH binding to VMAT2 and [^{3}H]DA uptake into rat synaptic vesicles with similar efficiency. Therefore, lobeline appears to specifically interact with the DTBZOH binding sites on VMAT2 to inhibit DA uptake into synaptic vesicles. On the other hand, *d*-amphetamine (*d*-AMPH) inhibits [^{3}H]DTBZOH binding to vesicle membranes 20 times more weakly than the inhibition of rVMAT2 function, suggesting that *d*-AMPH interacts with a different site than DTBZOH and lobeline on rVMAT2 to inhibit monoamine uptake. Furthermore, *d*-AMPH evoked [^{3}H]DA release is about 12 times more efficient than that of lobeline. Thus, in contrast to *d*-AMPH, which is equipotent in inhibiting DA uptake and promoting release from the synaptic vesicles, lobeline more potently (28-fold) inhibits DA uptake (*via* an interaction with the DTBZOH binding site on rVMAT2) than it evokes DA release to redistribute presynaptic DA storage [57].

Structurally modified lobeline derivatives, meso-transdiene (**69–71**) and lobelane (**72–76**) have been found to show high potency and selectivity for rVMAT2 relative to nicotinic receptor binding[58]. To establish the structure-activity relationships within, specific stereochemical forms of meso-transdiene, lobelane, and other structurally related analogs have been synthesized and evaluated for inhibition of [^{3}H]nicotine binding to α4β2* nAChR, [^{3}H]methyllycaconitine binding to α7* nAChR, and [^{3}H]DTBZOH binding to rVMAT2[59]. All these analogs showed lower affinities for α4β2* and α7* nAChRs compared to lobeline, thus increased selectivity for rVMAT2. Only modest loss of affinity for rVMAT2 in comparison to lobelane was observed by; (1) altering the stereochemistry at the C-2 and C-6 positions of the piperidine ring; (2) varying unsaturation in the piperidine C-2 and C-6 substituents; (3) introducing unsaturation into the piperidine ring; (4) ring-opening or eliminating the piperidine ring, and (5) removing the piperidine N-Me group. Incorporation of a quaternary ammonium group into defunctionalized lobeline molecules in

the *cis*-series resulted in significant loss of affinity for rVMAT2, whereas only a modest change in affinity was obtained in the *trans*-series. The most potent and rVMAT2-selective compounds were the bis 3′ fluorophenyl derivative (**75**) (570 nM) and N-methyl-2,6-cis-bis(naphthalene ethyl) piperidine analog (**76**), ($K_i = 630$ nM). Thus, the most promising structural changes to the lobeline molecule that enhance the rVMAT2 affinity and selectivity are defunctionalization, affording lobelane and meso-transdiene, and replacement of the phenyl rings of lobelane with other aromaticmoieties.

The benzofuran antiarrhythmic drug, amiodarone [Scheme 2 (**77**)], exhibits anti-adrenergic action in the heart, which resembles the effects of RES. The molecular origin of these apparent presynaptic, sympatholytic effects of amiodarone has been examined using Chinese hamster ovary (CHO) cells expressing VMAT2 as a synaptic vesicle model[60]. Amiodarone inhibit the uptake of [^{3}H]NE in VMAT2-transfected CHO cells in a concentration-dependent manner, with a -log EC_{50} of 6.4. [^{3}H]RES binding to the membrane fractions prepared from CHO cells expressing VMAT2 was inhibited by amiodarone in a concentration and pH independent manner, with a -log EC_{50} of 6.76, reaching 84% inhibition of RES binding at 10 μM. Therefore, amiodarone inhibits the uptake of monoamine into the storage vesicle by inhibiting the activity of VMAT2 and binds to the same site as RES. These findings suggest a novel presynaptic site of action for amiodarone *in vivo.*

5. Imaging Agents and Radio-ligands

Specific VMAT2 ligands with high affinity have been clinically useful imaging agents for early diagnosis and monitoring of the progression of neurodegenerative disease associated with the CNS monoaminergic system such as Parkinson's (PD) and Alzheimer's diseases (AD) (reviews)[61–63]. These imaging agents may also be important tools for exploiting the relationship between loss of insulin-secreting β-cells and onset of diabetes mellitus, since recent studies indicate that significant amounts of VMAT2 is also expressed in the β-cell mass (BCM) in the pancreas, mainly in the islets of Langerhans (review)[64]. Accordingly, high affinity VMAT2 inhibitors with ^{11}C, ^{3}H, ^{125}I, and ^{18}F labels have been synthesized, characterized, and tested in animals and humans as *in vivo* imaging agents. TBZ and related derivatives have been chosen as the prime candidates for these studies, probably due to their high and specific VMAT2 affinity and easy synthetic accessibility of suitable labels.

[^{11}C]Tetrabenazine ([^{11}C]TBZ)

[^{11}C]TBZ [Scheme 1 & Table VII (**5**)**;** label on the 9-O-CH$_3$) has been characterized as a positron emission tomography (PET) imaging reagent of VMAT2 in mice. After i.v. injection, [^{11}C]TBZ was rapidly taken up into the brain and quickly lost from most areas of the brain except from the striatum and hypothalamus which are rich in VMAT2[65]. The order of [^{11}C]TBZ binding at 10 min after injection was striatum > hypothalamus > hippocampus > cortex = cerebellum and parallel to the VMAT2 content of the tissues as determined by *in vitro* histochemical assays. The specificity of VMAT2 binding was confirmed by competition experiments with unlabeled TBZ and pretreatment of animals with RES and/or DA uptake inhibitor GBR 12935. Similar to the results of the studies with mice, [^{11}C]TBZ, showed high brain uptake and relatively slower clearance from regions of highest VMAT2 concentrations (striatum), resulting in clear differential visualization of these structures at short time intervals after the injection (10–20 min) in the living human brain[66]. In unilaterally MPTP-lesioned monkey, the specific binding of radio-ligand was absent in the striatum on the lesioned side, with no effect on radiotracer distribution in the cortex, cerebellum or contra lateral striatum[67]. These studies show that [^{11}C]TBZ can be used in *in vivo* PET imaging and semi quantitative determination of VMAT2 in the living human brain. However, detailed pharmacokinetic studies showed that [^{11}C]TBZ is rapidly converted to α- and β [^{11}C]dihydrotetrabenazine (DTBZOH) and to 9-O-desmethyl TBZ,

reducing *in vivo* accumulation in mouse striatum and hypothalamus. Therefore, quantitative pharmacokinetic modeling of radioactivity distribution would be complicated by the presence of these pharmacologically active metabolites of [^{11}C]TBZ[68].

[^{11}C]Dihydrotetrabenazine

As mentioned above the quantitative pharmacokinetic modeling of radioactivity distribution of [^{11}C]TBZ is complicated by its rapid *in vivo* conversion to pharmacologically active metabolites[68]. Therefore, the relatively metabolically inactive, potent VMAT inhibitor [^{11}C]DTBZOH (label on the 9-O-CH$_3$) has been characterized as a useful imaging agent [Table VII (**78**)]. The changes in the catecholaminergic areas of the brains of patients with multiple system atrophy, sporadic olivopontocerebellar atrophy and normal control subjects were determined and compared using [^{11}C]DTBZOH as a PET agent[69]. Specific binding of [^{11}C]DTBZOH in the striatum was significantly reduced in the multiple system atrophy patients as compared with the normal control group, in the caudate nucleus putamen. Smaller but significant reductions were observed in the sporadic olivopontocerebellar atrophy group, in the same areas. In another study, with PD significant reduction in specific [^{11}C]TBZOH binding in the putamen and in the caudate nucleus was observed[70]. A comparison of equilibrium to kinetic conditions in the analysis of PET data for the assessment of VMAT2 binding density using resolved active isomer, (+)-α-[^{11}C]dihydrotetrabenazine [(+)-α-[^{11}C]DTBZOH)], has also been reported[71]. A loading bolus followed by continuous infusion lead to a steady-state distribution of the label in both tissue and blood by 30 min, and the tissue-to-blood distribution ratios of (+)-α[^{11}C]DTBZOH) at equilibrium are in close agreement with the kinetic estimates. Thus, a simple, easily tolerated protocol using a loading bolus followed by continuous infusion can provide excellent measures of VMAT2 binding.

The striatal VMAT2 binding site density in a relatively large number of PD subjects (31 early stage PD subjects and 75 normal subjects) have been determined using (+)-α-[^{11}C]DTBZOH as a PET imaging agent employing continuous i.v. infusion with an equilibrium tracer modeling protocol[72]. In normal subjects age-related decline in striatal (+)-α-[^{11}C]DTBZOH binding was about 0.5% per year. In PD subjects, specific (+)-α-[^{11}C]DTBZOH binding was reduced significantly in the caudate nucleus, anterior putamen, and posterior putamen, and substantia nigra. These results demonstrate that (+)-α-[^{11}C]DTBZOH-PET imaging displays many properties necessary of a PD biomarker[73]. However, recent studies suggest that DA depleting drugs such as α-methyl-*p*-tyrosine, *d*-AMPH and the DA elevating agent γ-hydroxybutyrate alter striatal (+)-α-[^{11}C]DTBZOH binding in rats. Therefore, *in vivo* (+)-α[^{11}C]DTBZOH binding in imaging studies is subject to competition by vesicular DA and, in this respect, is not a "stable" DA biomarker as is generally assumed. Similarly, recent whole body biodistribution and dosimetry studies in baboons show most of the injected tracer [^{11}C]-DTBZOH localized to the liver and the lungs, followed by the intestines, brain, and kidneys[74]. The highest estimated absorbed radiation dose was in the stomach wall. Therefore, the dose estimates as well as the radiation dose to other radiosensitive organs, must be considered in evaluating the risks of multiple administrations of [^{11}C]-DTBZOH as a tracer.

α- [2-^{3}H]-dihydrotetrabenazine (DTBZOH)

Alpha-2-dihydrotetrabenazine [DTBZOH; Table VII (**78**)], a major metabolite of TBZ is also a potent inhibitor of VMAT2, similar to the parent compound. The tritiated derivative α-[2-^{3}H] dihydrotertabenazine [^{3}H]DTBZOH was the first radiotracer used for VMAT2 imaging, most likely due to its convenient synthetic accessibility[75]. Early studies showed that [^{3}H]DTBZOH binding in rat brain was stable up to 72 h of postmortem at 22°. [^{3}H]DTBZOH binding was specific, saturable (K$_d$ 2.7 nM) in major regions of post mortem

human brain and readily displaced by substrates or other inhibitors of VMAT2. The highest densities of binding sites were in regions of caudate nucleus, putamen, and accumbens nucleus of the CNS. [³H]DTBZOH binding in caudate nucleus and in putamen from normal postmortem human subjects is well correlated with the distribution of catecholamine metabolites[76]. Significant changes in [³H]DTBZOH binding levels were observed in PD and AD brains compared to the controls. A large decrease in [³H]DTBZOH binding was observed in all parts of the striatum in PD brains. These data corroborate the deficiency in striatal dopaminergic transmission in PD and agree with the notion that dopaminergic terminals have disappeared and/or no longer contain synaptic vesicles in PD brains. In AD brains, [³H]DTBZOH binding was significantly reduced in the ventral striatum and not in the caudate nucleus and putamen. The specific decrease of monoaminergic transporter levels in the ventral striatum suggests that this nucleus is a target area in AD. These findings suggest that [³H]DTBZOH is also a reliable *in vivo* imaging agent for VMAT2 and could be used to diagnose PD and AD in post mortem human brain.

α-[O-methyl] methoxytetrabenazine(MT BZ)

α-[2-O-methyl-³H]methoxytetrabenazine [Table VII (**80**); MTBZ] binding to the VMAT has also been studied in rat brain sections by autoradiography[77]. [³H]MTBZ interacts with a homogeneous population of striatal sites. Highest levels of [³H]MTBZ binding sites were in regions richly innervated by the monoamine systems and RES significantly inhibited [³H]MTBZ binding. Unilateral lesion of the median forebrain bundle with 6-hydroxydopamine reduces the [³H]MTBZ binding and the decrease correlated well with the reduction of tyrosine hydroxylase-positive neuron density in the substantia nigra pars compacta. Therefore, [³H]MTBZ is a reliable and quantitative tracer of VMAT2 which provides an accurate assessment of monoamine neuronal losses and may thus be of value in the diagnosis and study of neurodegenerative diseases.

The ¹¹C labeled α-[2-O-methyl-¹¹C]methoxytetrabenazine [¹¹C]MTBZ has also been tested as a tracer for VMAT2[78]. The highest activity of [¹¹C]MTBZ was observed in the striatum, lateral septum, substantia nigra pars compacta, the raphe nuclei and the locus coeruleus of rat brain after 15 min of injection which parallels the known monoamine nerve terminal density of the CNS. At this time interval, over 82% of brain activity, but less than 47% of plasma activity corresponded to authentic [¹¹C]MTBZ. [¹¹C]MTBZ binding in the mouse brain was inhibited by co-injection of excess unlabeled DTBZOH. In humans, initial brain uptake of [¹¹C]MTBZ was fast and rapidly cleared from all regions with longest retention times in areas of high VMAT2 concentration. Parametric quantification of VMAT2 density showed the highest distribution volume in the putamen and caudate with lower values in cerebral cortex and cerebellum. Acute treatments with RES, TBZ or related benzoisoquinolines significantly reduced [¹¹C]MTBZ binding *in vivo*[79]. However, radiotracer distributions remained unchanged after treatments with other dopaminergic drugs, haloperidol, pargyline, deprenyl, and L-DOPA Me ester. Repeated injections of TBZ did not alter the *in vivo* radio-ligand binding measured after allowing drug washout from the brain. These studies support the proposal that *in vivo* PET imaging of VMAT2 using [¹¹C]MTBZ in patients with extra pyramidal movement disorders will not be affected by concurrent use of L-DOPA or deprenyl. The usefulness of [¹¹C]MTBZ as a PET scanning agent was further studied by using a tottering mice model[80]. The distribution of [¹¹C]MTBZ in the brain regions of striatum, cortex, hippocampus, hypothalamus, cerebellum and thalamus of tottering mice was about 150–190% higher than that of the control aminals. This increase tissue distribution correlates well with the two to three fold increase of NE levels of these regions of brains of these mice in comparison to normal mice as previously determined by histochemical methods. While these results are consistent with the proposed noradrenergic hyper-innervation characteristic of the tottering mutant mouse, they further

confirm that [11C]MTBZ could be used satisfactorily to measure not only decrease in the density of VMAT, but also the increase in the transporter density in various catecholaminergic dysfunctions for diagnostic purposes. Therefore, [11C] MTBZ appears to be a suitable ligand for PET quantification of the VMAT in the human brain under various physiological conditions[80].

2-Iodovinyl Tetrabenazine (I-VTBZ)

A derivative of TBZ containing a 2-iodovinyl group [125I-VTBZ;Table VII (**87**)] was tested as a possible SPECT agent[81]. Following i.v. injection in rats, [125I]I-VTBZ readily crosses the blood brain barrier and localizes into the brain. However, distribution of the label was not specific to any region of the brain. One of the two resolved isomers of 125I-VTBZ showed more efficient uptake in comparison to the other, but still with a modest degree of specificity for the striatum. The binding of [125I]I-VTBZ could be blocked by pretreatment of rats with cold TBZ. In rat striatal homogenates, the more active isomer showed a pharmacological profile consistent with specific binding to VMAT2 sites. *In vitro* autoradiographic studies using rat brain sections further show that 125I-VTBZ predominantly labeled the regions rich in VMAT-2 sites. However, the low target-nontarget specificity ratio observed for this derivative (probably due to its high lipophilicity), makes it a poor candidate for *in vivo* imaging of VMAT2.

Fluoroalkyl Dihydro tetrabenazine Derivatives

To increase the availability of VMAT2 imaging agents for routine clinical studies with PET, 18F analogs of DTBZOH with a longer half-life ($t_{1/2}$ = 110 min compared 20 min for 11C) have been synthesized and characterized[86]. Racemic ($\pm$)-[18F]-fluoroethyl-DTBZOH (**88**) and ($\pm$)-[18F]-fluoropropyl-DTBZOH (**89**) were high affinity ligands for VMAT2 [K_is of 0.76 and 0.56 nM, respectively (Table VII)] in rat striatal homogenates, similar to the parent ($\pm$)-DTBZOH. *In vitro* **89** distinctly binds to the caudate putamen region consistent with the localization of VMAT2 in the mouse brain, which was blocked by nonradioactive TBZ efficiently. Both tracers show excellent brain uptakes on mice after an i.v. injection. The brain wash out of **89** was faster than **88** and thus **89** yielded a better target-to-background ratio. Therefore, the racemic **89** is potentially a useful imaging agent for VMAT2 binding sites in the brain. The specific binding and regional brain pharmacokinetics of **89** was also studied in the primate brain[87]. The brain uptakes and pharmacokinetics of **89** and (+)-[11C]DTBZOH were similar in the monkey brain. Metabolic defluorination was slow and minor for the [18F]fluoroalkyl-DTBZOH ligands. The (+)-**89** was the active isomer for VMAT2 inhibition with a K_i of 0.1 ± 0.01 in rat striatal homogenates (Table VII)[88]. The characteristics of high specific binding ratio, reversibility, metabolic stability and longer half-life of the radionuclide make (+)-**89** a promising alternative VMAT2 radio-ligand suitable for widespread use in human PET studies of monoaminergic innervations of the brain.

As mentioned above, imaging of pancreatic BCM using VMAT2 specific tracers may provide an important tool for understanding the relationship between loss of insulin-secreting β-cells and onset of diabetes mellitus. A PET study of BCM on the pancreas of Lewis rats using [11C]DTBZOH show that decreased radio-ligand uptake within the pancreas of Lewis rats with streptozotocin-induced diabetes relative to their euglycemic historical controls[89]. These initial studies strongly support the suggestion that the quantification of VMAT2 expression in β cells by PET represents a method for noninvasive longitudinal estimations of changes in BCM that may be useful in the study and treatment of diabetes. Recently, (+)-**89** was also evaluated as a PET agent for BCM *in vivo*. The pancreas taken up high levels of (+)-**89**, but VMAT2 inactive isomer, (−)-**89**, taken up only weakly[90]. The uptake was reduced by 78% in rats pretreated with unlabeled (+)-**89**. Therefore, (+)-**89**

could also be a useful PET agent for pancreatic β-cell mass. A new VMAT2 imaging agent, [^{18}F](+)-2-oxiranyl-3-isobutyl-9-(3-fluoropropoxy)-10-methoxy-2,3,4,6,7,11b-hexahydro-1H-pyrido[2,1-a]isoquinoline (**90**), was also evaluated as a PET agent for estimating beta cell mass *in vivo*[91]. The hydrolysable epoxide group of **90** was hypothesized to shift biodistribution from liver to kidney, thus reducing the background signal. The preliminary results suggest that **90** is highly selective in binding to VMAT2 and taken up into the pancreas of rats effectively and, the liver uptake was significantly reduced as expected. Therefore, **90** may potentially be a better imaging agent for β-cell mass of pancreas.

Other Ligands

KET, a known 5-HT2 receptor antagonist, is also a high-affinity ligand for VMAT2 of bovine chromaffin granules and synaptic vesicles (Table VIII). [^{3}H]KET [Scheme 1;(**7**)] binds to the same site as TBZ with a K_d of 6 nM at 0 °C and 45 nM at 30 °C[36] (Table VIII). 7-Amino 8-[^{125}I]ketanserin have been tested as a radio-tracer for VMAT in rat brain[92]. Although significant binding to the monoaminergic areas of the brain slices was observed, the non-specific binding was higher in comparison to [^{3}H]DTBZOH suggesting that TBZ derivatives are better markers for *in vitro* autoradiographic studies of monoaminergic neurons. However, the azido derivative, 7-azido-8- [^{125}I]ketanserin [Scheme 1 (**16**)] K_d for VMAT is 5.5 nM at 0 °C[93]] has been successfully used to photoaffinity label bovine chromaffin granules, human pheochromocytoma, rat striatum, and rabbit blood platelet VMATs[93]. This derivative has also been used to identify and purify the VMAT 2 from bovine adrenal chromaffin granule membranes.

Several other KET derivatives have been synthesized and their structure-activity relationships have been reported (Table VIII). These studies show that increasing the distance between the piperidine ring and the heterocyclic ring by two methylene units (**97**) reduces affinity for TBZ binding site of bVMAT2 by about 20 fold (K_i = 950 nM for [^{3}H]DTBZOH binding)[36] in comparison to the parent derivative. The reduction of benzyl carbonyl to an alcohol group (**93**) reduces the bVMAT2 affinity by about 9 fold (K_i = 350 nM for [^{3}H]DTBZOH binding). The alteration of the heterocyclic ring system with other heterocylces (**94–96**) also significantly reduces the affinity for TBZ binding site of bVMAT2[36]. These findings suggest that the structure of KET is somewhat optimal for the interaction with the TBZ binding site of bVMAT2.

6. Pharmacology

Effects of Amphetamines on VMAT

Neuropharmacological and neurotoxic effects of a number of illicit drugs and neurotoxins are closely associated with their interference with the physiological functions of VMATs. Increasing evidence suggests that cocaine and AMPH-related illicit drugs exert their effects by increasing the non-exocytotic release of DA in specific regions of the brain probably through direct modulation of VMAT2 functions[8–10]. This proposal is supported by the observation that multiple administrations of METH rapidly decreased vesicular DA uptake and DTBZOH binding, an effect that persist at least 24 h in rat brain[94]. Similar to METH, 3,4-methylelendioxy methamphetamine (MDMA) also rapidly decreased vesicular DA transport in striatal vesicles prepared from treated rats[95]. In contrast, treatment with DAT inhibitors (cocaine[96] or methylphenidate[97]) abruptly and reversibly increased both the V_{max} of DA uptake and the B_{max} for VMAT2 binding of DTBZOH, in purified rat striatal synaptic vesicles. Further studies with synaptosomal membranes and vesicle-enriched fractions prepared from drug treated rat brains show a differential redistribution of VMAT2 within striatal synaptic terminals upon drug treatment[98]. In particular, cocaine shifts

VMAT2 protein from a synaptosomal membrane fraction to a vesicle-enriched fraction, and in contrast, METH treatment redistributes VMAT2 from a vesicle-enriched fraction to a location that is not retained in synaptosomal preparations. These data suggest that the psychostimulants cocaine and METH acutely and differentially affect VMAT2 subcellular localization causing the perturbation of DA distribution in the cell in a contrasting manner. Further studies suggest that AMPH induced modulations of VMAT2 activity are mediated by a D2 receptor-associated pathway[99–101]. However, a recent study suggests that METH-mediated rapid decrease in the VMAT2 function in striatal DA terminals is a consequence of a neuronal nitric oxide synthase-dependent oxidation of VMAT2 and a long-term decrease in VMAT2 protein and function[102]. In addition, the surviving DA terminals after METH exposure may have a compromised capacity to buffer cytosolic DA concentrations and DA-derived oxidative stress.

The effects of amphetamines on the brains of human users have also been investigated. DA nerve terminal markers, DA, tyrosine hydroxylase, and DAT, were reduced in post-mortem striatum (nucleus accumbens, caudate, putamen) of chronic METH users[103]. Levels of DOPA decarboxylase and VMAT2 were normal in postmortem brains of young subjects suggesting that chronic exposure to METH does not cause permanent degeneration of striatal DA nerve terminals at the doses used by these young individuals. A recent immuno-histochemical study of post mortem brains of METH users also show a decrease in tyrosine hydroxylase in the nucleus accumbens and DAT in the nucleus accumbens and putamen. But no significant difference of VMAT2 was observed between METH and control groups. However, in this study, remarkably reduced VMAT2 levels were observed in the nucleus accumbens of METH users, in contrast to the previous study[104]. In addition, sustained, high dose METH exposures *in vivo*, reduce the striatal dopaminergic markers in rats suggesting a neurotoxic effect[105]. As opposed to other markers of striatal dopaminergic terminals, VMAT2 expression was not altered, under conditions dopaminergic transmission is altered without synaptic terminal losses. However, neurotoxic METH treatment reduced both striatal VMAT2 and DAT. Dopaminergic markers, DAT, VMAT2, and dopamine D1 and D2 receptors, were also significantly reduced in caudate-putamen of rats at 15 min or 6 days after chronic METH treatment for two months[106]. While dopamine D1 and D2 receptors fully recovered after 30 days of drug abstinence, DA and the DAT exhibited significant but incomplete recovery. In contrast, only the VMAT-2 exhibited no evidence of recovery over the 30-day withdrawal period which is in good agreement with the irreversible loss of the synaptic terminals.

The effects of repeated AMPH administration on the expression of DAT and VMAT2 genes have also been reported[107]. A significant increase (10–20% of the controls) in DAT mRNA levels was found in rostral portions of ventral tegmental area, substantia nigra and the transitional zone and in the intermediate portion of substantia nigra in rats 3 days after the 5 day treatment of AMPH. VMAT2 mRNA was significantly increased only in rostral and intermediate portions of the transitional zone. After 14 days of withdrawal, a statistically significant increase of DAT mRNA levels was observed only in the intermediate portion of ventral tegmental area, but no changes in VMAT2 mRNA levels. Therefore, repeated non-toxic doses of AMPH administration appear to exert modest and regionally selective effects on DAT and VMAT2 mRNA expression in subpopulations of midbrain DA neurons.

Effects of Cocaine on VMAT

Short-term (5 days) cocaine treatment is reported to increase the VMAT2 density in both prefrontal cortex and striatum of rat brain[108]. This could probably be a compensatory mechanism in place to maintain the vesicular monoamine storage capacity under the conditions where the cytosolic DA levels are depleted. However, further studies are necessary to confirm and fully exploit these findings. However, striatal DAT and VMAT2

protein levels were reduced in post mortem brains of cocaine users, similar to METH users[109]. A marked reduction in VMAT2 immunoreactivity and [³H]DTBZOH binding was observed in striatal samples of chronic cocaine users in comparison to age-, sex-, and postmortem interval-matched comparison subjects[110]. Subjects suffering from cocaine-induced mood disorders displayed a greater loss of VMAT2 immunoreactivity. The loss of VMAT2 protein reflects damage to striatal DA fibers of human cocaine users, which could play a role in causing disordered mood and motivational processes in more severely dependent patients. Therefore, the VMAT2 could be a valuable marker in the clinical study of cocaine neurotoxicity.

Studies with VMAT2 Knockout Mice

The physiological effects of VMAT2 malfunctions have also been studied using knockout mice models. Homozygous (VMAT2−/−)mice move little, feed poorly, and die within a few days after birth. Monoaminergic cells and their projections were indistinguishable from those of wild-type littermates, but the brains of mutant mice show a drastic reduction in monoamines[111]. Use of midbrain cultures from the mutant animals showed that AMPH but not depolarization induced DA release. *In vivo*, AMPH increased movement, promoted feeding, and prolonged the survival of VMAT2−/− animals, indicating that precise, temporally regulated exocytotic release of monoamines is not required for certain complex behaviors. The brains of VMAT2 heterozygotes (VMAT2 +/−) contained substantially lower monoamine levels than those of wild-type littermates, and depolarization induced less DA release from heterozygous than from wild-type cultures[111]. These changes in presynaptic homeostasis are accompanied by a pronounced super sensitivity of the mice to the locomotor effects of the DA agonist apomorphine, the psychostimulants cocaine and AMPH, and ethanol[112]. Importantly, VMAT2 heterozygous mice do not develop further sensitization to repeated cocaine administration. METH-induced dopaminergic neurotoxicity was increased in the striatum of VMAT2 +/− mice compared with wild-type. Interestingly, increased METH neurotoxicity in VMAT2 +/− mice was accompanied by a less pronounced increase in extracellular DA and indexes of free radical formation compared with wild-type mice[113]. Administration of the neurotoxin MPP⁺ precursor MPTP to heterozygotes produces more than twice the DA cell losses found in wild-type mice[114]. These observations stress the importance of VMAT2 in the maintenance of presynaptic function and suggest that VMAT2 +/− mice may provide an animal model for delineating the mechanisms of vesicular release, monoamine function, and postsynaptic sensitization associated with drug abuse and mechanism of action of certain neurotoxins.

Non-exocytotic Release of Catecholamines by Amphetamines

Mechanism of the non-exocytotic release of catecholamines by amphetamines and related derivatives is not fully understood at present. However, AMPH mediated disruption of the intragranular pH gradient has been proposed as a major contributing factor. AMPH and related derivatives are lipophilic weak bases (pKa 9.9)[115] and have been shown to nonspecifically diffuse through the plasma and vesicle membranes to accumulate in synaptic vesicles in large quantities. The unprotonated amine is protonated by the acidic environment of the vesicle resulting in the alkalinization of the granule matrix and dissipation of the catecholamine gradient. The high levels cytosolic catecholamines are effluxed through the plasma membrane amine transporters leading to depletion of catecholamine levels in the cell. Although this weak base hypothesis has been generally accepted, several other alternate mechanisms have also been proposed. For example, AMPH derivatives were also known to inhibit the vesicular [³H] DA uptake through VMAT2 without altering the [³H] DTBZOH binding capacity[116]. The VMAT2 inhibition could lead to an increase in cytosolic catecholamine levels resulting in increase of efflux through plasma membrane amine transporters. Similarly, study of a large number of AMPH and related derivatives show that

most of them are also VMAT2 substrates and they deplete vesicular neurotransmitter *via* a carrier-mediated exchange mechanism rather than *via* a weak base effect as commonly accepted[117]. The redistribution of VMAT2 from the granule membranes to a non-granular location by AMPH related derivatives leading to the increase of cytosolic catecholamines has also been proposed as the cause of the non-exocytotic release [118–119]. On the other hand, studies in hVMAT2 and hDAT transfected mammalian HEK293 cells show that preloaded [^{3}H] METH was retained more effectively by both hDAT and hDAT+hVMAT2 tranfected cells at higher extracellular pH (8.6) than lower pH (7.4)[120]. However, preloaded [^{3}H] DA was more effectively retained at lower pH than at higher pHs. Therefore, the back transport of DA and METH through the DAT and VMAT2 require different H$^+$ concentrations suggesting that two different mechanisms are involved in these two processes. Undoubtedly, additional experimental evidence is necessary to determine the exact mechanism of the depletion of intracellular catecholamines by AMPH and related derivatives.

VMAT, Perturbation of Catecholamine Metabolism, and Neurotoxicity

Increased cytosolic accumulation due to the perturbation of catecholamine accumulation into storage vesicles could cause increased oxidative stress and oxidative damage to the catecholaminergic neurons[121–123]. Therefore, VMAT inhibitors could be toxic to catecholaminergic neurons. In agreement with this notion, neurotoxicity of bVMAT2 inhibitors, 3-amino-2-phenylpropene (APP) derivatives in human neuroblastoma SH-SY5Y cells has been recently reported[124]. These derivatives are specifically toxic to SH-SY5Y, but not to non-neuronal M-1, HEPG-2 or HEK-293 cells at similar concentrations. However, they accumulate in all these cells through passive diffusion. They drastically perturb DA uptake and metabolism in SH-SY5Y cells under sub-lethal conditions, and are able to deplete both vesicular and cytosolic catecholamines similar to amphetamines. The treatment of SH-SY5Y cells with APP derivatives significantly increases intracellular ROS and decreases glutathione levels, and the cell death is significantly attenuated by the antioxidants α-tocopherol, *N*-acetyl-L-cysteine and glutathione, but not by the non-specific caspase inhibitor Z-VAD-FMK (carbobenzoxy-valyl-alanyl-aspartyl-[O-methyl]-fluoromethylketone). DNA fragmentation analysis supports that cell death is likely due to a caspase-independent ROS-mediated apoptotic pathway. Increased oxidative stress generated by the perturbation of DA metabolism has been proposed as the cause of apoptotic SH-SY5Y cell death[124].

The metabolite of 1-methyl-4-phenyl-1,2,3,6-tetrahydropyridine (MPTP), N-methyl-4-phenylpyridinium (MPP$^+$), selectively destroys dopaminergic neurons and induces the symptoms of Parkinson's disease in humans and other primates[125–130]. Specific dopaminergic toxicity of MPP$^+$ has been widely exploited to model the pathophysiology of Parkinson's disease[130–131]. Many important aspects of MPP$^+$ metabolism including *in vivo* and *in vitro* interactions with monoaminergic and other systems have been studied in great detail. Numerous studies have shown that MPP$^+$ is taken up into the dopaminergic neurons through DAT[132–134] and accumulated into storage vesicles through VMAT2[11–12,135]. MPP$^+$ has been shown to be a weak inhibitor of mitochondrial electron transport chain complex I[136–137]. Based on these and other evidence, specific uptake through DAT followed by the inhibition of mitochondrial complex I has been proposed as the major cause of specific dopaminergic toxicity of MPP$^{+138–139}$. According to this model, granular accumulation of MPP$^+$ through VMAT2 in dopaminergic neurons is proposed to be an effective *in vivo* detoxification mechanism[114]. Although the above proposals are supported by early observations, recent studies suggest that specific uptake through DAT or NET may not be necessary for MPP$^+$ toxicity. In contrast to previous reports, neuronal cell lines MN9D and SH-SY5Y as well as the non-neuronal cell line HEPG-2 take-up MPP$^+$ with similar efficiency[140]. Uptake of MPP$^+$ into SH-SY5Y cells is DAT and/or NET mediated,

whereas the uptake into other two cell lines are not mediated by DAT or NET, and appears to be mediated by a non-specific cation transporter. However, MPP[+] is only significantly toxic to MN9D cells, but not to SH-SY5Y or HEPG-2 cells. These findings, argue against a mechanism in which the specific dopaminergic toxicity of MPP[+] is due to the specific uptake through DAT followed by mitochondrial complex I inhibition. Similarly, based on these findings the proposal that VMAT2 mediated granular accumulation of cytosolic MPP[+] constitute a detoxification mechanism is also highly questionable, since HEPG-2 cells have no granulation mechanism. In agreement with these proposals, recent studies suggest that mitochondrial complex I inhibition may not be required for dopaminergic neuron death induced by MPP[+141]. Therefore, other mechanisms including interference of MPP[+] with intracellular catecholamine metabolism leading to high oxidative stress[142] should be considered as possible contributors for MPP[+] toxicity. More recent studies indicate that multiple mechanisms and pathways could be responsible for the neurotoxicity of MPP[+143–144]. Therefore, additional studies are necessary to firmly establish the specific dopaminergic toxicity of MPP[+].

7. Target for the Development of CNS Therapeutics

VMAT is solely responsible for the transport of cytoplasmic monoamines into synaptic vesicles for storage and subsequent exocytotic release in the central nervous system. The cytosolic accumulation of catecholamines could cause increased oxidative stress and oxidative damage to the catecholaminegic system potentially leading to neurodegenerative diseases[121–122]. Therefore, pharmacological enhancement of catecholamine sequestration into synaptic vesicles by VMAT2 could be a possible strategy for treating and/or preventing neurodegenerative diseases such as PD[145]. Several recent studies have attempted to provide experimental evidence for this proposal. For example, methylphenidate, a potent inhibitor of DAT and central nervous system stimulant, is widely used for the treatment of children and adults with attention deficit hyperactivity disorder. It is shown to increase DA levels in the brain and both DA content of the synaptic vesicles and K^{+}-stimulated DA release from striatal suspensions of rat brain due to the increased VMAT2 activity[146]. Methylphenidate has been also shown to be useful for ameliorating cognitive, affective, and motor deficits in PD and in other neurological patients. The increased synaptic vesicle concentration of DA has been proposed as a possible cause for these beneficial effects. Similarly, a number of studies have shown that pramipexole which is a dopamine D2/D3 receptor agonist is useful in the treatment of Parkinson's disease. Both human and animal studies suggest that pramipexole may also exhibit dopaminergic neuron protective properties[147]. Studies using synaptic vesicles prepared from striata of pramipexole treated rats show that pramipexole increases vesicular DA uptake through VMAT2. Similarly, nonselective dopamine D1/D2 receptor agonist apomorphine which is used to treat symptoms resulting from the dopaminergic degeneration associated with Parkinson's disease (in Europe) also show neuroprotective effects in rodent models. Interestingly, vesicular DA uptake was shown to be rapidly and reversibly increased in purified striatal vesicles obtained from apomorphine treated rats[148]. This increase was associated with a redistribution of VMAT2 protein within nerve terminals. The effect of apomorphine on vesicular DA uptake was blocked by pretreating the rats with eticlopride, a dopamine D2 receptor antagonist. Therefore, the neuroprotective effects of both pramipexole and apomorphine could be due to the increased sequestration into synaptic vesicles leading to the reduction of cytosolic DA levels.

A gents that reduced the dopaminergic neurotransmission have also been shown to lessen chorea associated with Huntington disease patients. Neuroleptics such as haloperidol have long been used for this purpose, but are associated with extrapyramidal side effects[149]. TBZ has also been long used for the treatment of chorea associated with Huntington disease in UK, Canada, and Australia[149–153] and has been recently approved in the US[154]. Although

the precise mechanism of the antichorea effects of TBZ is not clear, its ability to inhibit the VMAT2 resulting in the depletion of monoamines in the nerve terminals have been considered as a possibility[153].

VMAT2 has also been considered as a novel target for the development of treatments for psychostimulant abuse. VMAT2 inhibitors that are capable of inhibiting the psychostimulants mediated release of DA and the addiction liability may be efficacious for the treatment for METH abuse. For example, the VMAT2 inhibitor, lobeline has been shown to inhibit DA uptake into storage vesicles by interacting with the TBZ-binding site of VMAT2[155]. It also inhibits the promotion of DA release from the storage vesicles within the presynaptic terminal by AMPH and METH. In addition, lobeline was found to inhibit the AMPH-induced hyperactivity, drug discrimination, and self-administration. Thus, lobeline may reduce the abuse liability of these psychostimulants. Therefore, lobeline and lobeline analogs as well as other agents with targeted selectivity at VMAT2 represent a novel class of therapeutic agents potentially efficacious for the treatment of METH abuse. VMAT2 is also a newly emerging target for both diagnostic and therapeutic applications in diabetes mellitus. Recently, novel VMAT2 antagonists with dihydropyridone scaffold have been identified as potent hypoglycemic agent s[156–157].

8. VMAT and CNS Disorders

The notion that increased cytosolic DA lead to dopaminergic cell death in PD also suggests that regulatory polymorphisms in VMAT2 which affect its quantitative expression might serve as genetic risk factors for PD. Screening of the promoter region of the gene for VMAT2 (SLC18A2) has identified several polymorphisms that form discrete haplotypes. Several common haplotypes in SLC18A2 were found to involve gain-of-function and display significantly increased transcriptional activity from the reference element[158]. These gain-of-function haplotypes were tested for association with PD and found to confer a protective effect that was selective for females. This finding is consistent with the prediction that increased sequestration of DA in secretory vesicles by VMAT2 is protective for PD. Although these findings are consistent with the above proposals, additional direct experimental evidence is necessary for their conformation. In addition, several reports indicate that DNA polymorphisms located in SLC18A2 might also contribute to the development of nicotine and alcohol dependence[159–160].

Studies with the Flinders sensitive line (FSL) rats, which represent a genetic animal model for clinical depression in humans, suggest that alterations in VMAT2 may also play a role in the etiology of depression[161]. Reduced VMAT2 levels were determined in the striatum and its sub-regions, shell of nucleus accumbens but not in the core, the ventral tegmental area, and the substantia nigra pars compacta in FSL rats as measured by [^{3}H]DTBZOH binding. The reduced levels of VMAT2 protein were not accompanied by a parallel alteration in VMAT2 mRNA levels. Therefore, the activity of VMAT2 in FSL rat brain is not altered at the expression level, but at the functional level. Therefore, further studies at the molecular level are certainly necessary to fully describe these observations.

The VMAT1 gene SLC18A1 maps to chromosome 8p21.3, a locus with strong evidence of linkage with schizophrenia. An initial study reported that a non-synonymous single nucleotide polymorphism (SNP) of the VMAT1 gene (Pro4Thr) was associated with schizophrenia[162]. However, later studies found that there was no significant difference in genotype or allele distribution of the three SNPs of Pro4Thr, Thr136Ile, or Val392Leu between schizophrenia patients and controls of Japanese descent[163]. On the other hand, there was a significant difference in genotype and allele distributions for the Thr98Ser polymorphism between the two groups. The Thr98Ser allele was more common in female

patients than in male. Therefore, Thr98Ser polymorphism of VMAT1 was proposed to increase the susceptibility to schizophrenia in Japanese women. A study with 62 patients with schizophrenia and 188 control subjects of all European descent[164] show that the frequency of the minor allele of the Thr4Pro polymorphism was significantly increased in schizophrenia patients when compared to controls which were in agreement with the original study of Bly[162]. Assuming a recessive mode of inheritance, the frequency of homozygote 4Pro carriers was significantly increased in the schizophrenia patients when compared to controls. These results suggest that variations in the VMAT1 gene may confer susceptibility to schizophrenia in patients of European descent. In another study, genotypes of 585 patients with bipolar disorder type I and 563 control subjects, all of European descent[165] were obtained for three missense single nucleotide polymorphisms (Thr4Pro, Thr98Ser, Thr136Ile). Allele frequencies differed significantly for the potential functional polymorphism Thr136Ser between bipolar disorder patients and controls. Expression analysis confirmed that VMAT1 is expressed in human brain at the mRNA and protein level. Results suggest that variations in the VMAT1 gene may confer susceptibility to bipolar disorder in patients of European descent. In a recent study the hypothesis that the missense variation Thr136Ile in the VMAT1/SLC18A1 gene is associated with anxiety-related personality traits was tested in a total of 337 unrelated subjects of German descent (167 male, 170 female). Genotypes were obtained for the Thr136Ile variation in the VMAT1 gene for all subjects[166]. These studies also found that anxiety-related personality traits are associated with variation in the VMAT1/SLC18A1 gene. Therefore, cleanly, the exact nature of the polymorphism of the VMAT1/SLC18A1 gene that may confer susceptibility to schizophrenia, bipolar disorder type I, and anxiety-related personality traits appears to be dependent on the ethnicity of the subjects[167]. However, most available experimental data suggest that VMAT1 gene or certain regions of it may constitute a genetic susceptibility for schizophrenia, bipolar disorder, and other anxiety-related personality disorders. Further studies are necessary to confirm these findings and determine the role of VMAT1 in these disorders.

Conclusions

Significant progress has been made during the last 30 years on the understanding of the structure-function, pharmacology, and medicinal chemistry of VMAT. The critical role of VMAT is not only in sorting out, storing, and releasing of monoamine neurotransmitters, but also in protecting them from autooxidation has been well established. Interference with VMAT2 function has been proposed as one of the major causes of the neurotoxicity of psychostimulants and other toxins. Specific expression of VMAT2 in the CNS has been exploited in the development of useful radio-imaging agents for clinical diagnosis and management of neurodegenerative diseases such as Parkinson's disease. These imaging agents are also useful tools for exploiting the relationship between loss of insulin-secreting β-cells and onset of diabetes mellitus, since significant amounts of VMAT2 is also expressed in the β-cell mass (BCM) in the pancreas. The pharmacological modulation of the *in vivo* activity of VMAT2 has been considered as a potential strategy for the treatment of drug addiction and neuroprotection in neurodegenerative diseases. On the other hand, in spite of extensive efforts, the understanding of the structure-function relations of VMAT is lagging behind, primarily due to the lack of solid structural information. The tissue and species specific expression of two distinct VMAT isoforms or the regulation of their expression in various tissues has not been completely elucidated. Although very preliminary evidence suggest that the VMAT1 gene constitutes a genetic susceptibility for schizophrenia, bipolar disorder, and other anxiety-related personality disorders, further studies are certainly necessary to confirm these findings. Future efforts should be directed toward advancing these less developed areas to fully appreciate the vital role of VMAT in CNS functions and dysfunctions.

Acknowledgments

References

1. Henry J-P, Sagne C, Bedet C, Gasnier B. The vesicular Monoamine Transporter: from Chromaffin Granule to Brain. Neurochem Int. 1998; 32:227–246. [PubMed: 9587917]

2. Schuldiner S, Shirvan A, Linial M. Vesicular Neurotransmitter Transporters: From Bacteria to Humans. Physiol Rev. 1996; 75:369–392. [PubMed: 7724667]

3. Rudnick G. Bioenergetics of Neurotransmitter Transport. J Bioenerg Biomembr. 1998; 30:173–185. [PubMed: 9672239]

4. Eiden LE, Schäfer MK, Weihe E, Schütz B. The vesicular amine transporter family (SLC18): amine/proton antiporters required for vesicular accumulation and regulated exocytotic secretion of monoamines and acetylcholine. Pflugers Arch. 2004; 447:636–640. [PubMed: 12827358]

5. Schuldiner S. A molecular glimpse of vesicular monoamine transporters. J Neurochem. 1994; 62:2067–2078. [PubMed: 7910628]

6. Gasnier B. The loading of neurotransmitters into synaptic vesicles. Biochimie. 2000; 82(4):327–337. [PubMed: 10865121]

7. Henry J-P, Botton D, Sagne C, Isambert M-F, Desnos C, Blanchard V, Raisman-Vozari R, Krejci E, Massoulie J, Gasnier B. Biochemistry and Molecular Biology of the Vesicular Monoamine Transporter from Chromaffin Granules. J Exp Biol. 1994; 196:251–262. [PubMed: 7823026]

8. Schuldiner S, Steiner-Mordoch S, Yelin R, Wall SC, Rudnick C. Amphetamine Derivatives Interact with Both Plasma Membrane and Secretory Vesicle Biogenic Amine Transporters. Mol Pharmacol. 1993; 44(6):1227–1231. [PubMed: 7903417]

9. Volz TJ, Hanson GR, Fleckenstein AE. The role of the plasmalemmal dopamine and vesicular monoamine transporters in methamphetamine-induced dopaminergic deficits. J Neurochem. 2007; 101(4):883–888. [PubMed: 17250674]

10. Fleckenstein AE, Volz TJ, Riddle EL, Gibb JW, Hanson GR. New insights into the mechanism of action of amphetamines. Ann Rev Pharmacol Toxicol. 2007; 47:681–698. [PubMed: 17209801]

11. Daniels AJ, Reinhard JF Jr. Energy-driven Uptake of the Neurotoxin 1-Methyl-4-phenylpyridinium into Chromaffin Granules *Via* the Catecholamine Transporter. J Biol Chem. 1988; 263:5034–5036. [PubMed: 3258595]

12. Darchen F, Scherman D, Henry J-P. Characteristics of the Transport of Quaternary Ammonium 1-Methyl-4-phenylpyridinium by Chromaffin Granules. Biochem Pharmacol. 1988; 37:4381–4387. [PubMed: 3264161]

13. Lotharius J, O'Malley KL. The parkinsonism-inducing drug 1-methyl-4-phenylpyridinium triggers intracellular dopamine oxidation. A novel mechanism of toxicity. J Biol Chem. 2000; 275:38581–38588. [PubMed: 10969076]

14. German DC, Sonsalla PK. A role for the vesicular monoamine transporter (VMAT2) in Parkinson's disease. Adv Behavioral Biol. 2003; 54:131–137.

15. Liu Y, Peter D, Rogahani A, Schuldiner S, Prive GG, Eisenberg D, Brecha N, Edwards RH. A cDNA that Suppresses MPP^+ Toxicity Encodes a Vesicular Amine Transporter. Cell. 1992; 70:539–551. [PubMed: 1505023]

16. Erickson JD, Eiden LE. Functional identification and molecular cloning of a human brain vesicle monoamine transporter. J Neurochem. 1993; 61:2314–2317. [PubMed: 8245983]

17. Erickson JD, Eiden LE, Hoffman BJ. Expression cloning of a reserpine-sensitive vesicular monoamine transporter. Proc Natl Acad Sci USA. 1992; 89:10993–10997. [PubMed: 1438304]

18. Peter D, Liu Y, Sternini C, de Giorgio R, Brecha N, Edwards RH. Differential Expression of two Vesicular Monoamine Transporters. J Neuroscience. 1995; 15:6197–6188.

19. Weihe E, Schafer MKH, Erickson JD, Eiden LE. Localization of Vesicular Monoamine Transporter Isoforms (VMAT-1 and VMAT-2) to Endocrine Cells and Neurons in Rat. J Mol Neuroscience. 1995; 5:149–164.

20. Erickson JD, Schafer MKH, Bonner TI, Eiden LE, Weihe E. Distinct Pharmacological Properties and Distribution in Neurons and Endocrine Cells of Two Isoforms of the Human Vesicular Monoamine Transporter. Proc Natl Acad Sc USA. 1996; 93:5166–5171. [PubMed: 8643547]

21. Hansson SR, Mezey E, Hoffman BJ. Ontogeny of vesicular monoamine transporter mRNAs VMAT1 and VMAT2. II. Expression in neural crest derivatives and their target sites in the rat. Brain Res Dev Brain Res. 1998; 110:159–174.

22. Howell M, Shirvan A, Stern-Bach Y, Steiner-Mordoch S, Strasser JE, Dean GE, Schuldiner S. Cloning and functional expression of a tetrabenazine sensitive vesicular monoamine transporter from bovine chromaffin granules. FEBS Lett. 1994; 338:16–22. [PubMed: 8307150]

23. Krejci E, Gasnier B, Botton D, Isambert MF, Sagné C, Gagnon J, Massoulié J, Henry JP. Expression and regulation of the bovine vesicular monoamine transporter gene. FEBS Lett. 1993; 335:27–32. [PubMed: 7902299]

24. Parsons SM. Transport mechanisms in acetylcholine and monoamine storage. FASEB J. 2000; 14:2423–2434. [PubMed: 11099460]

25. Bravo D, Parsons SM. Microscopic kinetics and structure-function analysis in the vesicular acetylcholine transporter. Neurochem Int. 2002; 41:285–289. [PubMed: 12176068]

26. Hofmann K, Stoffel WA. database of membrane spanning proteins segments Biol. Chem Hoppe-Seyler. 1993; 374:166.

27. Njus D, Kelley PM, Harnadek GJ. Bioenergetics of secretory vesicles. Biochim Biophys Acta. 1986; 853:237–265. [PubMed: 2887202]

28. Kirshner N. Uptake of catecholamines by a particulate fraction of the adrenal medulla. J Biol Chem. 1962; 237:2311–2317. [PubMed: 14456353]

29. Knoth J, Zallakian M, Njus D. Stoichiometry of H^+-linked dopamine transport in chromaffin granule ghosts. Biochemistry. 1981; 20:6625–6629. [PubMed: 6458332]

30. Darchen F, Scherman D, Henry JP. Reserpine binding to chromaffin granules suggests the existence of two conformations of the monoamine transporter. Biochemistry. 1989; 28:1692–1697. [PubMed: 2719928]

31. Henry JP, Sagné C, Botton D, Isambert MF, Gasnier B. Molecular pharmacology of the vesicular monoamine transporter. Adv Pharmacol. 1998; 42:236–239. [PubMed: 9327887]

32. Knoth J, Isaacs JM, Njus D. Amine transport in chromaffin granule ghosts. pH dependence implies cationic form is translocated. J Biol Chem. 1981; 256(13):6541–3. [PubMed: 7240227]

33. Wimalasena DS, Wimalasena K. Kinetic evidence for channeling of dopamine between monoamine transporter and membranous dopamine-beta-monooxygenase in chromaffin granule ghosts. J Biol Chem. 2004; 279:15298–15304. [PubMed: 14732710]

34. Scherman D, Jaudon P, Henry JP. Characterization of the monoamine carrier of chromaffin granule membrane by binding of [2-3H]dihydrotetrabenazine. Proc Natl Acad Sci USA. 1983; 80:584–588. [PubMed: 6572908]

35. Scherman D, Henry JP. Reserpine binding to bovine chromaffin granule membranes. Characterization and comparison with dihydrotetrabenazine binding. Mol Pharmacol. 1984; 25:113–122. [PubMed: 6708929]

36. Darchen F, Scherman D, Laduron PM, Henry JP. Ketanserin binds to the monoamine transporter of chromaffin granules and of synaptic vesicles. Mol Pharmacol. 1988; 33:672–677. [PubMed: 3380081]

37. Slotkin TA, Seidler FJ, Whitmore WL, Lau C, Salvaggio M, Kirksey DF. Ratbrain synaptic vesicles: uptake specificities of [3H]norepinephrine and [3H]serotonin in preparations from whole brain and brain regions. J Neurochem. 1978; 31:961–968. [PubMed: 702157]

38. Disbrow JK, Ruth JA. Greatly extended viability of rat brain storage vesicles in an intracellular medium based upon a non-permeant polyanion. Life Sci. 1981; 29:1989–1996. [PubMed: 7311730]

39. Pothos EN, Larsen KE, Krantz DE, Liu Y, Haycock JW, Setlik W, Gershon MD, Edwards RH, Sulzer D. Synaptic vesicle transporter expression regulates vesicle phenotype and quantal size. J Neurosci. 2000; 20:7297–7306. [PubMed: 11007887]

40. Sulzer D, Pothos EN. Regulation of quantal size by presynaptic mechanisms. Rev Neurosci. 2000; 11:159–212. [PubMed: 10718152]

41. Peter D, Jimenez J, Liu Y, Kim J, Edwards RH. The chromaffin granule and synaptic vesicle amine transporters differ in substrate recognition and sensitivity to inhibitors. J Biol Chem. 1994; 269:7231–7237. [PubMed: 8125935]

42. Gasnier B, Krejci E, Botton D, Massoulie J, Henry JP. Expression of a bovine vesicular monoamine transporter in COS cells. FEBS Lett. 1994; 342:225–229. [PubMed: 8150075]

43. Shirvan A, Laskar O, Steiner-Mordoch S, Schuldiner S. Histidine-419 plays a role in energy coupling in the vesicular monoamine transporter from rat. FEBS Lett. 1994; 356:145–150. [PubMed: 7988710]

44. Steiner-Mordoch S, Shirvan A, Schuldiner S. Modification of the pH profile and tetrabenazine sensitivity of rat VMAT1 by replacement of aspartate 404 with glutamate. J Biol Chem. 1996; 271:13048–13054. [PubMed: 8662678]

45. Merickel A, Kaback HR, Edwards RH. Charged residues in transmembrane domains II and XI of a vesicular monoamine transporter form a charge pair that promotes high affinity substrate recognition. J Biol Chem. 1997; 272:5403–5408. [PubMed: 9038139]

46. Finn JP III, Edwards RH. Individual residues contribute to multiple differences in ligand recognition between vesicular monoamine transporters 1 and 2. J Biol Chem. 1997; 272:16301–16307. [PubMed: 9195934]

47. Finn JP III, Edwards RH. Multiple residues contribute independently to differences in ligand recognition between vesicular monoamine transporters 1 and 2. J Biol Chem. 1998; 273:3943–3947. [PubMed: 9461580]

48. Thiriot DS, Ruoho AE. Mutagenesis and derivatization of human vesicle monoamine transporter 2 (VMAT2) cysteines identifies transporter domains involved in tetrabenazine binding and substrate transport. J Biol Chem. 2001; 276:27304–27315. [PubMed: 11375404]

49. Thiriot DS, Sievert MK, Ruoho AE. Identification of Human Vesicle Monoamine Transporter (VMAT2) Lumenal Cysteines That Form an Intramolecular Disulfide Bond. Biochemistry. 2002; 41:6346–6353. [PubMed: 12009896]

50. Sagne C, Isambert M-F, Vandekerckhove J, Henry JP, Gasnier B. The Photoactivatable Inhibitor 7-Azido-8-iodoketanserin Labels the N Terminus of the Vesicular Monoamine Transporter from Bovine Chromaffin Granules. Biochemistry. 1997; 36:3345–3352. [PubMed: 9116013]

51. Sievert MK, Ruoho AE. Peptide mapping of the [^{125}I]iodoazidoketanserin and [125I]2-N-[(3′-iodo-4′-azidophenyl)propionyl]tetrabenazine binding sites for the synaptic vesicle monoamine transporter. J Biol Chem. 1997; 272:26049–26055. [PubMed: 9325342]

52. Gopalakrishnan A, Sievert M, Ruoho AE. Identification of the substrate binding region of vesicular monoamine transporter-2 (VMAT-2) using iodoaminoflisopolol as a novel photoprobe. Mol Pharmacol. 2007; 72:1567–1575. [PubMed: 17766642]

53. Perera RP, Wimalasena DS, Wimalasena K. Characterization of a Series of 3-Amino-2-phenylpropene Derivatives as Novel Bovine Chromaffin Vesicular Monoamine Transporter Inhibitors. J Med Chem. 2003; 46:2599–2605. [PubMed: 12801224]

54. Moriyama Y, Amakatsu K, Futai M. Uptake of the neurotoxin, 4-methylphenylpyridinium into chromaffin granules and synaptic vesicles: a proton gradient drives its uptake through monoamine transporter. Arch Biochem and Biophy. 1993; 305:271–277.

55. Wimalasena DS, Perera RP, Heyen BJ, Balasooriya IS, Wimalasena K. Vesicular monoamine Transporter Substrate/Inhibitor Activity of MPTP/MPP$^+$ Derivatives: A Structure-Activity Study. J Med Chem. 2008; 51:760–768. [PubMed: 18220329]

56. Chaplin L, Cohen AH, Huettl P, Kennedy M, Njus D, Temperley SJ. Reserpic acid as an inhibitor of norepinephrine transport into chromaffin vesicle ghosts. J Biol Chem. 1985; 260:10981–10985. [PubMed: 4030777]

57. Teng L, Crooks PA, Dwoskin LP. Lobeline displaces [^{3}H]dihydrotetrabenazine binding and releases [^{3}H]dopamine from rat striatal synaptic vesicles: comparison with *d*-amphetamine. J Neurochem. 1998; 71:258–265. [PubMed: 9648873]

58. Miller DK, Crooks PA, Zheng G, Grinevich VP, Norrholm SD, Dwoskin LP. Lobeline analogs with enhanced affinity and selectivity for plasmalemma and vesicular monoamine transporters. J Pharmacol Exp Ther. 2004; 310:1035–1045. [PubMed: 15121762]

59. Zheng G, Dwoskin LP, Deaciuc AG, Norrholm SD, Crooks PA. Defunctionalized Lobeline Analogues: Structure-Activity of Novel Ligands for the Vesicular Monoamine Transporter. J Med Chem. 2005; 48:5551–5560. [PubMed: 16107155]

60. Haikerwal D, Dart AM, Little PJ, Kaye DM. Identification of a novel, inhibitory action of amiodarone on vesicular monoamine transport. J Pharmacol Exp Ther. 1999; 288:834–837. [PubMed: 9918596]

61. Efange SMN. In vivo imaging of the vesicular acetylcholine transporter and the vesicular monoamine transporter. FASEB J. 2000; 14:2401–2413. [PubMed: 11099458]

62. Frey KA, Koeppe RA, Kilbourn MR. Imaging the vesicular monoamine transporter. Adv Neurol. 2001; 86:237–247. [PubMed: 11553983]

63. Guilloteau D, Chalon S. PET and SPECT exploration of central monoaminergic transporters for the development of new drugs and treatments in brain disorders. Curr Pharm Des. 2005; 11:3237–3245. [PubMed: 16250852]

64. Maffei A, Harris PE. Targeting vesicular monoamine transporter type 2 for noninvasive PET-based β-cell mass measurements. Expert Review of Endocrinology & Metabolism. 2007; 2:35–46.

65. DaSilva JN, Kilbourn MR. In vivo binding of [11C]tetrabenazine to vesicular monoamine transporters in mouse brain. Life Sci. 1992; 51:593–600. [PubMed: 1640810]

66. Kilbourn MR, DaSilva JN, Frey KA, Koeppe RA, Kuhl DE. In vivo imaging of vesicular monoamine transporters in human brain using [11C]tetrabenazine and positron emission tomography. J Neurochem. 1993; 60:2315–2318. [PubMed: 8492135]

67. Dasilva JN, Kilbourn MR, Domino EF. In vivo imaging of monoaminergic nerve terminals in normal and MPTP-lesioned primate brain using positron emission tomography (PET) and [11C]tetrabenazine. Synapse. 1993; 14:128–131. [PubMed: 8332945]

68. Dasilva JN, Carey JE, Sherman PS, Pisani TJ, Kilbourn MR. Characterization of [11C]Tetrabenazine as an in vivo radioligand for the vesicular monoamine transporter. Nucl Med Biol. 1994; 21:151–156. [PubMed: 9234277]

69. Gilman S, Frey KA, Koeppe RA, Junck L, Little R, Vander Borght TM, Lohman M, Martorello S, Lee LC, Jewett DM, Kilbourn MR. Decreased striatal monoaminergic terminals in olivopontocerebellar atrophy and multiple system atrophy demonstrated with positron emission tomography. Ann Neurol. 1996; 40:885–892. [PubMed: 9007093]

70. Frey KA, Koeppe RA, Kilbourn MR, Vander Borght TM, Albin RL, Gilman S, Kuhl DE. Presynaptic monoaminergic vesicles in Parkinson's disease and normal aging. Ann Neurol. 1996; 40:873–884. [PubMed: 9007092]

71. Koeppe RA, Frey KA, Kume A, Albin R, Kilbourn MR, Kuhl DE. Equilibrium versus compartmental analysis for assessment of the vesicular monoamine transporter using (+)-α-[11C]dihydrotetrabenazine (DTBZ) and positron emission tomography. J Cerebral Blood Flow and Metabolism. 1997; 17:919–931.

72. Bohnen NI, Albin RL, Koeppe RA, Wernette KA, Kilbourn MR, Minoshima S, Frey KA. Positron emission tomography of monoaminergic vesicular binding in aging and parkinson disease. Journal Cereb Blood Flow Metab. 2006; 26:1198–1212.

73. Tong J, Wilson AA, Boileau I, Houle S, Kish SJ. Dopamine modulating drugs influence striatal (+)-[11C]DTBZ binding in rats: VMAT2 binding is sensitive to changes in vesicular dopamine concentration. Synapse. 2008; 62:873–876. [PubMed: 18720517]

74. Murthy R, Harris P, Simpson N, van Heertum R, Leibel R, Mann JJ, Parsey R. Whole body [11C]-dihydrotetrabenazine imaging of baboons: biodistribution and human radiation dosimetry estimates. Eur J Nucl Med Mol Imaging. 2008; 35:790–797. [PubMed: 18060547]

75. Scherman D, Raisman R, Ploska A, Agid Y. [3H]Dihydrotetrabenazine, a new in vitro monoaminergic probe for human brain. J of Neurochem. 1988; 50:1131–1136. [PubMed: 3346671]

76. Lehericy S, Brandel J-P, Hirsch EC, Anglade P, Villares J, Scherman D, Duyckaerts C, Javoy-Agid F, Agid Y. Monoamine vesicular uptake sites in patients with Parkinson's disease and Alzheimer's disease, as measured by tritiated dihydrotetrabenazine autoradiography. Brain Res. 1994; 659:1–9. [PubMed: 7820649]

77. Vander Borght TM, Sima AAF, Kilbourn MR, Desmond TJ, Kuhl DE, Frey KA. [^{3}H]Methoxytetrabenazine: a high specific activity ligand for estimating monoaminergic neuronal integrity. Neuroscience. 1995; 68:955–962. [PubMed: 8577387]

78. Vander Borght TM, Kilbourn MR, Koeppe RA, DaSilva JN, Carey JE, Kuhl DE, Frey KA. In vivo imaging of the brain vesicular monoamine transporter. J Nucl Med. 1995; 36:2252–2260. [PubMed: 8523116]

79. Kilbourn MR, Frey KA, Borght TV, Sherman PS. Effects of dopaminergic drug treatments on in vivo radioligand binding to brain vesicular monoamine transporters. Nucl Med Biol. 1996; 23:467–471. [PubMed: 8832701]

80. Kilbourn MR, Sherman PS, Abbott LC. Mutant mouse strains as models for in vivo radiotracer evaluations: [11C]methoxytetrabenazine ([^{11}C]MTBZ) in tottering mice. Nucl Med Biol. 1995; 22:565–567. [PubMed: 7581164]

81. Canney DJ, Guo YZ, Kung MP, Kung HF. Synthesis and preliminary evaluation of an iodovinyl-tetrabenazine analog as a marker for the vesicular monoamine transporter. J Labelled Compd Radiopharm. 1993; 33:355–368.

82. DaSilva JN, Kilbourn MR, Mangner TJ. Synthesis of a [^{11}C]methoxy derivative of alpha-dihydrotetrabenazine: a radioligand for studying the vesicular monoamine transporter. Appl Radiat Isot. 1993; 44:1487–1489. [PubMed: 7903060]

83. Saner A, Pletscher A. A benzo[a]quinolizine derivative with a neuroleptic-like action on cerebral monoamine turnover. J Pharmacol Exp Ther. 1977; 203:556–563. [PubMed: 21955]

84. Kung MP, Canney DJ, Frederick D, Zhuang Z, Billings JJ, Kung HF. Binding of ^{125}I-iodovinyltetrabenazine to CNS vesicular monoamine transportsites. Synapse. 1994; 18:225–232. [PubMed: 7855735]

85. Lee LC, Vander Borght T, Sherman PS, Frey KA, Kilbourn MR. In vitro and in vivo studies of benzisoquinoline ligands for the brain synaptic vesicle monoamine transporter. J Med Chem. 1996; 39:191–196. [PubMed: 8568807]

86. Goswami R, Ponde DE, Kung MP, Hou C, Kilbourn MR, Kung HF. Fluoroalkyl derivatives of dihydrotetrabenazine as positron emission tomography imaging agents targeting vesicular monoamine transporters. Nucl Med Biol. 2006; 33:685–694. [PubMed: 16934687]

87. Kilbourn MR, Hockley B, Lee L, Hou C, Goswami R, Ponde DE, Kung MP, Kung HF. Pharmacokinetics of [^{18}F]fluoroalkyl derivatives of dihydrotetrabenazine in rat and monkey brain. Nucl Med Biology. 2007; 34:233–237.

88. Kung MP, Hou C, Goswami R, Ponde DE, Kilbourn MR, Kung HF. Characterization of optically resolved 9-fluoropropyl-dihydrotetrabenazine as a potential PET imaging agent targeting vesicular monoamine transporters. Nucl Med Biol. 2007; 34(3):239–246. [PubMed: 17383573]

89. Simpson NR, Souza F, Witkowski P, Maffei A, Raffo A, Herron A, Kilbourn MR, Jurewicz A, Herold K, Liu E, Hardy MA, Van Heertum R, Harris PE. Visualizing pancreatic β-cell mass with [^{11}C]DTBZ. Nucl Med Biol. 2006; 33:855–864. [PubMed: 17045165]

90. Kung MP, Hou C, Lieberman BP, Oya S, Ponde DE, Blankemeyer E, Skovronsky D, Kilbourn MR, Kung HF. In vivo imaging of β-cell mass in rats using 18F-FP-(+)-DTBZ: a potential PET ligand for studying diabetes mellitus. J Nucl Med. 2008; 49:1171–1176. [PubMed: 18552132]

91. Kung HF, Lieberman BP, Zhuang ZP, Oya S, Kung MP, Choi SR, Poessl K, Blankemeyer E, Hou C, Skovronsky D, Kilbourn MR. In vivo imaging of vesicular monoamine transporter 2 in pancreas using an (18)F epoxide derivative of tetrabenazine. Nucl Med Biol. 2008; 35:825–837. [PubMed: 19026944]

92. Darchen F, Masuo Y, Vial M, Rostene W, Scherman D. Quantitative autoradiography of the rat brain vesicular monoamine transporter using the binding of [^{3}H]dihydrotetrabenazine and 7-amino-8-[^{125}I]iodoketanserin. Neuroscience. 1989; 33:341–349. [PubMed: 2622531]

93. Isambert MF, Gasnier B, Laduron PM, Henry JP. Photoaffinity labeling of the monoamine transporter of bovine chromaffin granules and other monoamine storage vesicles using 7-azido-8-[^{125}I]iodoketanserin. Biochemistry. 1989; 28:2265–2270. [PubMed: 2719952]

94. Brown JM, Hanson GR, Fleckenstein AE. Methamphetamine rapidly decreases vesicular dopamine uptake. J Neurochem. 2000; 74:2221–2223. [PubMed: 10800970]

95. Hansen JP, Riddle EL, Sandoval V, Brown JM, Gibb JW, Hanson GR, Fleckenstein AE. Methylenedioxymethamphetamine decreases plasmalemmal and vesicular dopamine transport: mechanisms and implications for neurotoxicity. J Pharmacol Exp Ther. 2002; 300:1093–1100. [PubMed: 11861820]

96. Brown JM, Hanson GR, Fleckenstein AE. Regulation of the vesicular monoamine transporter-2: a novel mechanism for cocaine and other psychostimulants. J Pharmacol Exp Ther. 2000; 296:762–767. [PubMed: 11181904]

97. Sandoval V, Riddle EL, Hanson GR, Fleckenstein AE. Methylphenidate alters vesicular monoamine transport and prevents methamphetamine-induced dopaminergic deficits. J Pharmacol Exp Ther. 2003; 304:1181–1187. [PubMed: 12604695]

98. Riddle EL, Topham MK, Haycock JW, Hanson GR, Fleckenstein AE. Differential trafficking of the vesicular monoamine transporter-2 by methamphetamine and cocaine. Eur J Pharmacol. 2002; 449:71–74. [PubMed: 12163108]

99. Brown JM, Hanson GR, Fleckenstein AE. Cocaine-induced increases in vesicular dopamine uptake: role of dopamine receptors. J Pharmacol Exp Ther. 2001; 298:1150–1153. [PubMed: 11504813]

100. Fleckenstein AE, Brown JM, Sandoval V, Riddle EL, Hansen JP, Ugarte YV, Gibb JW, Hanson GR. D2 receptor-mediated regulation of vesicular dopamine uptake. Adv Behav Biol. 2002; 53:39–42.

101. Ugarte YV, Rau KS, Riddle EL, Hanson GR, Fleckenstein AE. Methamphetamine rapidly decreases mouse vesicular dopamine uptake: role of hyperthermia and dopamine D2 receptors. Eur J Pharmacol. 2003; 472:165–171. [PubMed: 12871750]

102. Eyerman DJ, Yamamoto BK. A rapid oxidation and persistent decrease in the vesicular monoamine transporter 2 after methamphetamine. J Neurochem. 2007; 103:1219–1227. [PubMed: 17683483]

103. Wilson JM, Kalasinsky KS, Levey AI, Bergeron C, Reiber AI, Bergeron C, Reiber G, Anthony RM, Schmunk GA. Striatal dopamine nerve terminal markers in human, chronic methamphetamine users. Nature Med. 1996; 2:699–703. [PubMed: 8640565]

104. Kitamura O, Tokunaga I, Gotohda T, Kubo S. Immunohistochemical investigation of dopaminergic terminal markers and caspase-3 activation in the striatum of human methamphetamine users. Int J Legal Med. 2007; 121:163–168. [PubMed: 16622715]

105. Frey K, Kilbourn MR, Robinson T. Reduced striatal vesicular monoamine transporters after neurotoxic but not after behaviorally-sensitizing doses of methamphetamine. Eur J Pharmacol. 1997; 334:273–279. [PubMed: 9369358]

106. Segal DS, Kuczenski R, O'Neil ML, Melega WP, Cho AK. Prolonged exposure of rats to intravenous methamphetamine: behavioral and neurochemical characterization. Psychopharmacology. 2005; 180:501–512. [PubMed: 15959831]

107. Lu W, Wolf ME. Expression of dopamine transporter and vesicular monoamine transporter 2 mRNAs in rat midbrain after repeated amphetamine administration. Mol Brain Res. 1997; 49:137–148. [PubMed: 9387873]

108. Schwartz K, Nachman R, Yossifoff M, Sapir R, Weizman A, Rehavi M. Cocaine, but not amphetamine, short term treatment elevates the density of rat brain vesicular monoamine transporter 2. J Neural Transm. 2007; 114:427–430. [PubMed: 16897597]

109. Wilson JM, Levey AI, Bergeron C, Kalasinsky K, Ang L, Peretti F, Adams VI, Smialek J, Anderson WR. Striatal dopamine, dopamine transporter, and vesicular monoamine transporter in chronic cocaine users. Ann Neurol. 1996; 40:428–439. [PubMed: 8797532]

110. Little KY, Krolewski DM, Zhang L, Cassin BJ. Loss of striatal vesicular monoamine transporter protein (VMAT2) in human cocaine users. The Am J Psychiat. 2003; 160:47–55.

111. Fon EA, Pothos EN, Sun BC, Killeen N, Sulzer D, Edwards RH. Vesicular transport regulates monoamine storage and release but is not essential for amphetamine action. Neuron. 1997; 19:1271–1283. [PubMed: 9427250]

112. Wang YM, Gainetdinov RR, Fumagalli F, Xu F, Jones SR, Bock CB, Miller GW, Wightman RM, Caron MG. Knockout of the vesicular monoamine transporter 2 gene results in neonatal death

and supersensitivity to cocaine and amphetamine. Neuron. 1997; 19:1285–1296. [PubMed: 9427251]

113. Fumagalli F, Gainetdinov RR, Wang YM, Valenzano KJ, Miller GW, Caron MG. Increased methamphetamine neurotoxicity in heterozygous vesicular monoamine transporter 2 knock-out mice. J Neuroscience. 1999; 19:2424–2431.

114. Takahashi N, Miner LL, Sora I, Ujike H, Revay RS, Kostic V, Jackson-Lewis V, Przedborski S, Uhl GR. VMAT2 knockout mice: heterozygotes display reduced amphetamine-conditioned reward, enhanced amphetamine locomotion, and enhanced MPTP toxicity. Proc Natl Acad Sci USA. 1997; 94:9938–9943. [PubMed: 9275230]

115. Sulzer D, Rayport S. Amphetamine and other psychostimulants reduce pH gradients in midbrain dopaminergic neurons and chromaffin granules: a mechanism of action. Neuron. 1990; 5:797–808. [PubMed: 2268433]

116. Schwartz K, Weizman A, Rehavi M. The effect of psychostimulants on [3H]dopamine uptake and release in rat brain synaptic vesicles. J Neural Transm. 2006; 113:1347–1352. [PubMed: 16362637]

117. Partilla JS, Dempsey AG, Nagpal AS, Blough BE, Baumann MH, Rothman RB. Interaction of amphetamines and related compounds at the vesicular monoamine transporter. J Pharmacol Exp Ther. 2006; 319:237–246. [PubMed: 16835371]

118. Brown JM, Hanson GR, Fleckenstein AE. Methamphetamine Rapidly Decreases Vesicular Dopamine Uptake. J Neurochem. 2000; 74:2221–2223. [PubMed: 10800970]

119. Riddle EL, Topham MK, Haycock JW, Hanson GR, Fleckenstein AE. Differential trafficking of the vesicular monoamine transporter-2 by methamphetamine and cocaine. Eur J Pharmacol. 2002; 449:71–74. [PubMed: 12163108]

120. Wilhelm CJ, Johnson RA, Eshleman AJ, Janowsky A. Hydrogen ion concentration differentiates effects of methamphetamine and dopamine on transporter-mediated efflux. J Neurochem. 2006; 96:1149–1159. [PubMed: 16417578]

121. Cohen G, Kesler N. Monoamine oxidase and mitochondrial respiration. J Neurochem. 1999; 73:2310–2315. [PubMed: 10582588]

122. Liu Y, Edwards RH. The role of vesicular transport proteins in synaptic transmission and neural degeneration. Annu Rev Neurosci. 1997; 20:125–156. [PubMed: 9056710]

123. Adams JD Jr, Chang ML, Klaidman L. Parkinson's disease--redox mechanisms. Curr Med Chem. 2001; 8:809–814. [PubMed: 11375751]

124. Samms WC, Perera RP, Wimalasena DS, Wimalasena K. Perturbation of dopamine metabolism by 3-amino-2-(4′-halophenyl)propenes leads to increased oxidative stress and apoptotic SH-SY5Y cell death. Mol Pharmacol. 2007; 72:744–752. [PubMed: 17576792]

125. Langston JW, Ballard P, Tetrud JW, Irwin I. Chronic Parkinsonism in humans due to a product of meperidine-analog synthesis. Science. 1983; 219:979–980. [PubMed: 6823561]

126. Burns RS, Chiueh CC, Markey SP, Ebert MH, Jacobowitz DM, Kopin IJ. Primate model of parkinsonism: Selective destruction of dopaminergic neurons in the pars compacta of the substantia nigra by N-methyl-4-phenyl-1,2,3,6-tetrahydropyridine. Proc Natl Acad Sci USA. 1983; 80:4546–4550. [PubMed: 6192438]

127. Markey SP, Johannessen JN, Chiueh CC, Burns RS, Herkenham MA. Intraneuronal generation of a pyridinium metabolite may cause drug-induced parkinsonism. Nature. 1984; 311:464–467. [PubMed: 6332988]

128. Heikkila RE, Manzino L, Cabbot FS, Duvoisin RC. Protection against the dopaminergic neurotoxicity of 1-methyl-4-phenyl-1,2,5,6-tetrahydropyridine by monoamine oxidase inhibitors. Nature. 1984; 311:467–469. [PubMed: 6332989]

129. Langston JW, Irwin I, Langston EB. Pargyline prevents MPTP-induced parkinsonism in primates. Science. 1984; 225:1480–1482. [PubMed: 6332378]

130. Bradbury AJ, Costall B, Domeney AM, Jenner P, Kelly ME, Marsden CD, Naylor RJ. 1 -Methyl-4-phenylpyridine is neurotoxic to the nigrostriatal dopamine pathway. Nature. 1986; 319:56–57. [PubMed: 3484542]

131. Bové J, Prou D, Perier C, Przedborski S. Toxin-induced models of Parkinson's disease. NeuroRx. 2005; 2:484–494. [PubMed: 16389312]

132. Javitch JA, D'Amato RJ, Strittmatter SM, Snyder SH. Parkinsonism-inducing neurotoxin, N-methyl-4-phenyl-1,2,3,6 -tetrahydropyridine: uptake of the metabolite N-methyl-4-phenylpyridine by dopamine neurons explains selective toxicity. Proc Natl Acad Sci USA. 1985; 82:2173–2177. [PubMed: 3872460]

133. Storch A, Ludolph AC, Schwarz J. Dopamine transporter: involvement in selective dopaminergic neurotoxicity and degeneration. J Neural Transm. 2004; 111:1267–1286. [PubMed: 15480838]

134. Gainetdinov RR, Fumagalli F, Jones SR, Caron MG. Dopamine transporter is required for in vivo MPTP neurotoxicity: evidence from mice lacking the transporter. J Neurochem. 1997; 69:1322–1325. [PubMed: 9282960]

135. Reinhard JF Jr, Diliberto EJ Jr, Viveros OH, Daniels AJ. Subcellular compartmentalization of 1-methyl-4-phenylpyridinium with catecholamines in adrenal medullary chromaffin vesicles may explain the lack of toxicity to adrenal chromaffin cells. Proc Natl Acad Sci USA. 1987; 84:8160–8164. [PubMed: 2891137]

136. Nicklas WJ, Vyas I, Heikkila RE. Inhibition of NADH-linked oxidation in brain mitochondria by 1-methyl-4-phenyl-pyridine, a metabolite of the neurotoxin, 1-methyl-4-phenyl-1,2,5,6-tetrahydropyridine. Life Sci. 1985; 36:2503–2508. [PubMed: 2861548]

137. Ramsay RR, Salach JI, Singer TP. Uptake of the neurotoxin 1-methyl-4-phenylpyridine (MPP$^+$) by mitochondria and its relation to the inhibition of the mitochondrial oxidation of NAD$^+$-linked substrates by MPP$^+$ Biochem Biophys Res Commun. 1986; 134:743–748. [PubMed: 2868716]

138. Lin MT, Beal MF. Mitochondrial dysfunction and oxidative stress in neurodegenerative diseases. Nature. 2006; 443:787–895. [PubMed: 17051205]

139. Fornai F, Schlüter OM, Lenzi P, Gesi M, Ruffoli R, Ferrucci M, Lazzeri G, Busceti CL, Pontarelli F, Battaglia G, Pellegrini A, Nicoletti F, Ruggieri S, Paparelli A, Südhof TC. Parkinson-like syndrome induced by continuous MPTP infusion: convergent roles of the ubiquitin-proteasome system and alpha-synuclein. Proc Natl Acad Sci USA. 2005; 102:3413–3418. [PubMed: 15716361]

140. Wimalasena K, Le V. Unpublished observations.

141. Choi W-S, Kruse SE, Palmiter RD, Xia Z. Mitochondrial complex I inhibition is not required for dopaminergic neuron death induced by rotenone, MPP$^+$, or paraquat. Proc Natl Acad Sci USA. 2008; 105:15136–15141. [PubMed: 18812510]

142. Obata T. Dopamine efflux by MPTP and hydroxyl radical generation. J Neural Transm. 2002; 109:1159–80. [PubMed: 12203043]

143. Wang J, Xu Z, Fang H, Duhart HM, Patterson TA, Ali SF. Gene expression profiling of MPP(+)-treated MN9D cells: A mechanism of toxicity. Neurotoxicology. 2007; 28:979–987. [PubMed: 17475336]

144. Xu Z, Patterson TA, Wren JD, Han T, Shi L, Duhart H, Ali SF, Slikker W Jr. A microarray study of MPP$^+$-treated PC12 Cells: Mechanisms of toxicity (MOT) analysis using bioinformatics tools BMC. Bioinformatics. 2005; 6 (Suppl 2):S8. [PubMed: 16026605]

145. Zheng G, Dwoskin LP, Crooks PA. Vesicular monoamine transporter 2: role as a novel target for drug development. AAPS J. 2006; 8:E682–692. [PubMed: 17233532]

146. Auriel E, Hausdorff JM, Giladi N. Methylphenidate for the treatment of Parkinson disease and other neurological disorders. Clin Neuropharmacol. 2009; 32:75–81. [PubMed: 18978488]

147. Truong JG, Rau KS, Hanson GR, Fleckenstein AE. Pramipexole increases vesicular dopamine uptake: implications for treatment of Parkinson's neurodegeneration. Eur J Pharmacol. 2003; 474:223–226. [PubMed: 12921866]

148. Truong JG, Hanson GR, Fleckenstein AE. Apomorphine increases vesicular monoamine transporter-2 function: implications for neurodegeneration. Eur J Pharmacol. 2004; 492:143–147. [PubMed: 15178358]

149. Grimbergen YA, Roos RA. Therapeutic options for Huntington's disease. Curr Opin Investig Drugs. 2003; 4:51–54.

150. Quinn GP, Shore PA, Brodie BB. Biochemical and pharmacological studies of RO 1-9569 (tetrabenazine), a nonindole tranquilizing agent with reserpine-like effects. J Pharmacol Exp Ther. 1959; 127:103–109. [PubMed: 14435563]

151. Dalby MA. Effect of tetrabenazine on extrapyramidal movement disorders. Br Med J. 1969; 2:422–423. [PubMed: 4238453]

152. Ondo WG, Tintner R, Thomas M, Jankovic J. Tetrabenazine treatment for Huntington's disease-associated chorea. Clin Neuropharmacol. 2002; 25:300–302. [PubMed: 12469001]

153. Marshall FJ, Walker F, Frank S, Oakes D, Plumb S, Factor SA, Fahn S, Hunt VP, Jankovic J, Shinaman A, Shoulson I. Tetrabenazine as antichorea therapy in Huntington's disease: a randomized controlled trial. Neurology. 2006; 66:366–372. [PubMed: 16476934]

154. Food and Drug Administration. FDA labeling information. FDA web site (online) http://www.accessdata.fda.gov/drugsatfda_docs/label/2008/021894lbl.pdf

155. Dwoskin LP, Crooks PA. A novel mechanism of action and potential use for lobeline as a treatment for psychostimulant abuse. Biochem Pharmacol. 2002; 63:89–98. [PubMed: 11841781]

156. Xie Y, Raffo A, Ichise M, Deng S, Harris PE, Landry DW. Novel hypoglycemic dihydropyridones serendipitously discovered from O- versus C-alkylation in the synthesis of VMAT2 antagonists. Bioorg Med Chem Lett. 2008; 18:5111–5114. [PubMed: 18752945]

157. Harris, P.; Xie, Y.; Landry, D.; Deng, SX.; Maffei, A. Methods and compositions using a vesicular monoamine transporter type 2 (VMAT2) antagonist for modulating insulin secretion and glucose metabolism. PCT Int Appl. WO 2008-US3338 20080312. 2008. Application

158. Glatt CE, Wahner AD, White DJ, Ruiz-Linares A, Ritz B. Gain-of-function haplotypes in the vesicular monoamine transporter promoter are protective for Parkinson disease in women. Hum Mol Genet. 2006; 15:299–305. [PubMed: 16339215]

159. Schwab SG, Franke PE, Hoefgen B, Guttenthaler V, Lichtermann D, Trixler M, Knapp M, Maier W, Wildenauer DB. Association of DNA polymorphisms in the synaptic vesicular amine transporter gene (SLC18A2) with alcohol and nicotine dependence. Neuropsychopharmacology. 2005; 30:2263–2268. [PubMed: 15988470]

160. Lin Z, Walther D, Yu XY, Li S, Drgon T, Uhl GR. SLC18A2 promoter haplotypes and identification of a novel protective factor against alcoholism. Hum Mol Genet. 2005; 14:1393–1404. [PubMed: 15829504]

161. Schwartz K, Yadid G, Weizman A, Rehavi M. Decreased limbic vesicular monoamine transporter 2 in a genetic rat model of depression. Brain Res. 2003; 965:174–179. [PubMed: 12591135]

162. Bly M. Mutation in the vesicular monoamine gene, SLC18A1, associated with Shizophrenia. Schizophr Res. 2005; 78:337–338. [PubMed: 15961286]

163. Richards M, Iijima Y, Kondo H, Shizuno T, Hori H, Arima K, Saitoh O, Kunugi H. Association study of the vesicular monoamine transporter 1 (VMAT1) gene with schizophrenia in a Japanese population. Behav Brain Funct. 2006; 2:39. [PubMed: 17134514]

164. Lohoff FW, Weller AE, Bloch PJ, Buono RJ, Doyle GA, Ferraro TN, Berrettini WH. Association between polymorphisms in the vesicular monoamine transporter 1 gene (VMAT1/SLC18A1) on chromosome 8p and schizophrenia. Neuropsychobiology. 2008; 57:55–60. [PubMed: 18451639]

165. Lohoff FW, Dahl JP, Ferraro TN, Arnold SE, Gallinat J, Sander T, Berrettini WH. Variations in the Vesicular Monoamine Transporter 1 Gene (VMAT1/SLC18A1) are Associated with Bipolar I Disorder. Neuropsychopharmacology. 2006; 31:2739–2747. [PubMed: 16936705]

166. Lohoff FW, Lautenschlager M, Mohr J, Ferraro TN, Sander T, Gallinat J. Association between variation in the vesicular monoamine transporter 1 gene on chromosome 8p and anxiety-related personality traits. Neurosci Lett. 2008; 434:41–45. [PubMed: 18249496]

167. Gutierrez B, Rosa A, Papiol S, Arrufat FJ, Catalan R, Salgado P, Peralta V, Cuesta MJ, Fananas L. Identification of two risk haplotypes for schizophrenia and bipolar disorder in the synaptic vesicle monoamine transporter gene (SVMT). Am J Med Genet B Neuropsychiatr Genet. 2007; 144B:502–507. [PubMed: 17427184]

168. Zheng G, Dwoskin LP, Deaciuc AG, Zhu J, Jones MD, Crooks PA. Lobelane analogues as novel ligands for the vesicular monoamine transporter-2. Bioorg Med Chem. 2005; 13:3899–3909. [PubMed: 15911306]

Biography

Kandatege Wimalasena, Ph. D. is currently a Professor of Chemistry at Wichita State University. He received his B. Sc (Hon.) degree in Chemistry from the University of Peradeniya, Sri Lanka, in 1977. After the first degree, he worked as a temporary assistant lecturer at the Department of Biochemistry, University of Colombo, Sri Lanka, until 1981. He obtained his Ph. D. in Chemistry/Biochemistry from the department of chemistry, Georgia Institute of Technology in 1986. The main focus of his graduate studies was in the broad area of mechanistic studies of monooxygenase catalysis, particularly dopamine β-monooxygenase. He was a post doctoral fellow at Georgia Tech. from 1986–1989 and studied the catecholamine metabolism in resealed bovine adrenal chromaffin granule ghosts. He joined the department of chemistry at Wichita State University in 1989. His current research interests include catecholamine metabolism, oxidative stress and neurodegeneration.
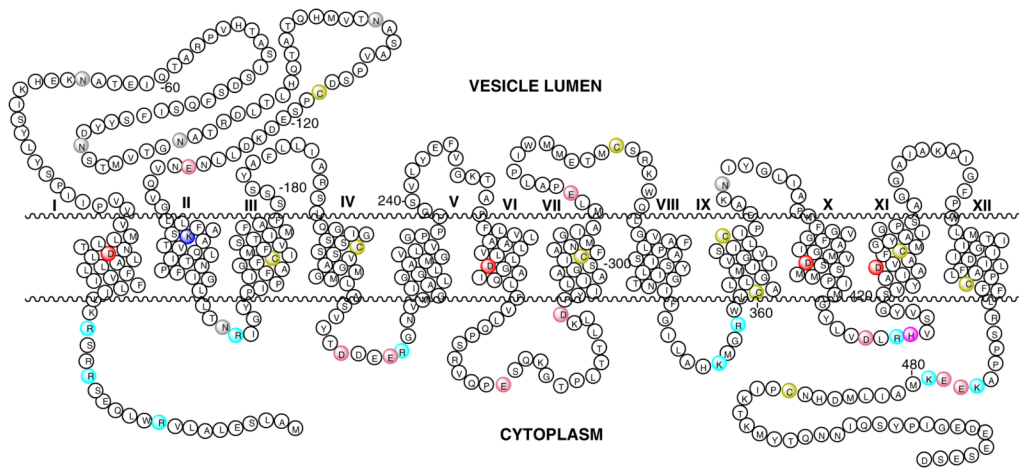
**Fig. 1. Predicted Secondary Structure of hVMAT2**
The structure is predicted by using TMbase - A database of membrane spanning protein
segments[26]. Conserved (in hVMAT1, hVMAT2, rVMAT1, rVMAT2, and bVMAT2)
transmembrane ● Asp 33, 262, 399, 426, and ●Lys 138; proposed vesicle lumen disulfide
bridged ●* Cys 117, and 324; and glycosylation sites ● Asn are shown. The conserved ●
Cys (117, 302, 324, 360, 374, 430, 467, and 488); cytoplasmic domain charged residues ●
Lys (354, 476, and 479), ●Arg (10, 16, 19, 155, 217, 357,413), ● Glu (216, 278, 477, and
478), ● Asp (213, 291, and 411) and ● His 414, and vesicle luman ● Glu (127 and 312)are
also shown (amino acid numbering is based on the sequence of hVMAT2).
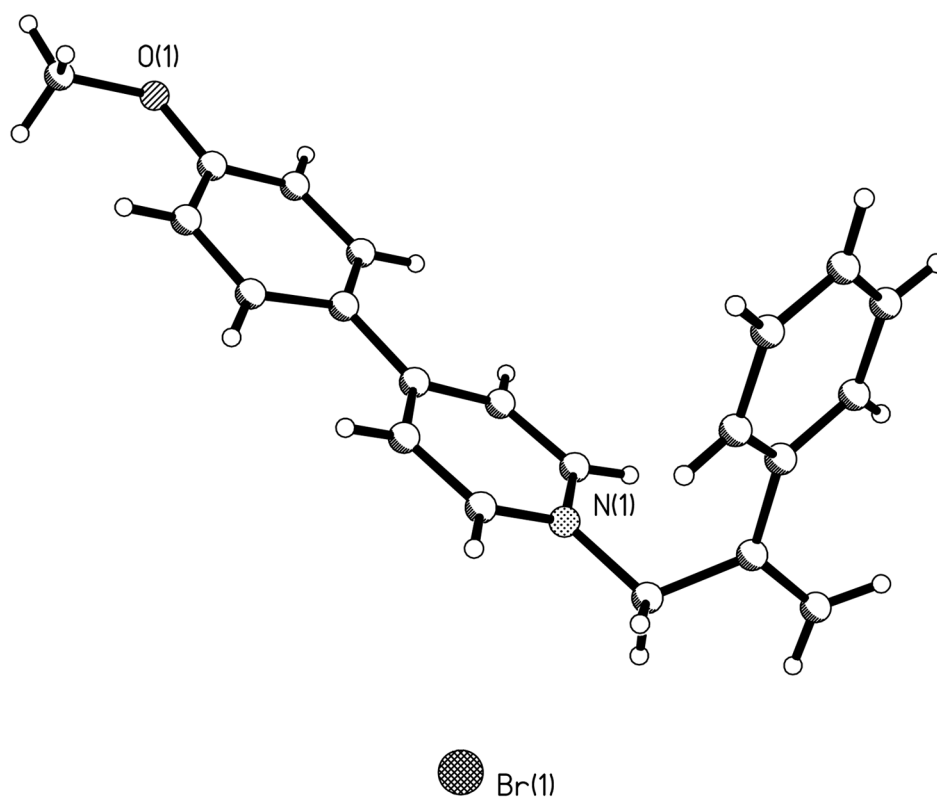
Figure 2.
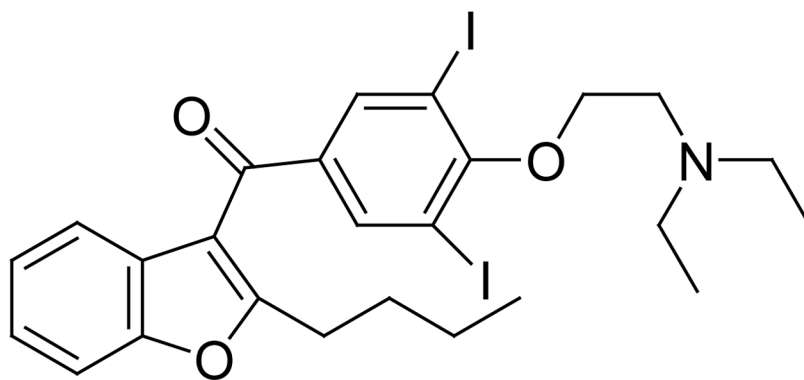Crystal structure of MPP$^+$-APP conjugate **64**.
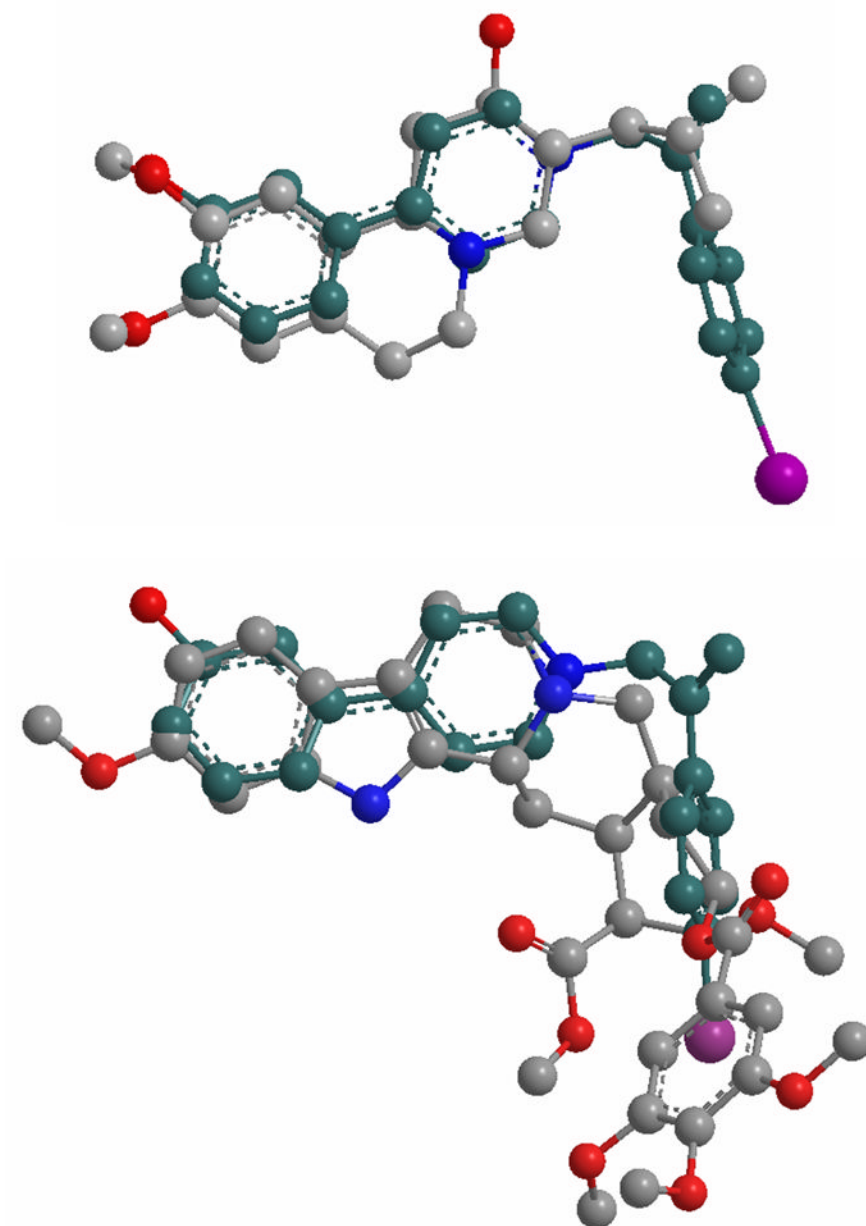
Figure 3.
Overlay of energy minimized structures of Tetrabenazine with **65** (*top*), and Reserpine with **65** (*bottom*).
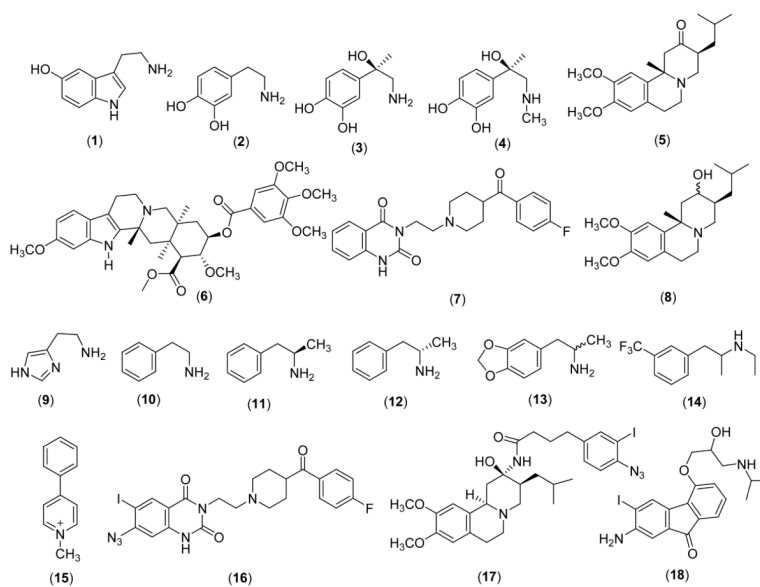
Scheme 1.
Structures of Common VMAT Substrates and Inhibitors

(**77**)

Scheme 2.

Table I

Uptake and Inhibition Kinetic Parameters of Resealed Bovine Chromaffin Granule Ghosts/Membranes

	Substrate/Inhibitor	K_m or K_I (µM)	V_{max} (nmoles/min.mg)	K_D (nM)	Ref.
1	5HT	19 ± 4	1.6 ± 1.0		32a
2	DA	25 ± 7	$0.8 \pm .5$		32a
		23.8 ± 1.5	1.60 ± 0.03		33b
3	NE	91.5 ± 10.5	0.95 ± 0.05		33c
4	E	68.4 ± 4.7	1.13 ± 0.03		33c
5	TBZ	3.2×10^{-3}		1.3	34c
6	RES	10×10^{-3}		0.3 ± 0.2 (I)	35d
				18 ± 10 (II)	
7	KET			45 ± 2.4	36e
8	TBZOH	3.7×10^{-3}		2.9	34c
				5.8 ± 1.0	35d
16				5.5×10^{-3}	93f

[a] Determined using resealed granule ghosts using [3H]5HT and [3H]DA in the presence of 100 mM ATP, at pH 7.2[32].

[b] Determined with resealed granule ghosts using non-radioactive substrates with HPLC-EC in the presence of 10 mM ATP, at pH 7.2[33].

[c] Determined with [3H]TBZ and [3H]TBZOH at 25 °C[34] using bovine granule membranes.

[d] Determined with [3H]TBZOH and [3H]reserpine (sites I & II) using bovine chromaffin granule membrens[35].

[e] Determined with [3H]KET at 30 °C using granule memebranes[36].

[f] K_d determined using [3H] ketanserin at 0° C and chromaffin granule memebranes[93].

Table II

Relative Inverse Affinities of Substrates and Inhibitors of VMAT in Heterologous Expression Systems

	Substrate/Inhibitor	hVMAT1[a]	hVMAT2[a]	rCGVMAT[b]	bVMAT2[c]	Chromaffin Granules[d]
1	5HT	1.4 ± 0.2	0.9 ± 0.1	0.85 ± 0.023	0.59	0.4
2	DA	3.8 ± 0.4	1.4 ± 0.2	1.56 ± 0.035	1.4	-
3	NE	13.7 ± 1.6	3.4 ± 0.5	2.5 ± 0.04	1.7	1.4
4	E	5.5 ± 0.7	1.9 ± 0.2	1.86 ± 0.011	2.5	1.4
5	Tetrabenazine(TBZ)	>20	0.097 ± 0.002		0.027	
6	Reserpine (RES)	0.034 ± 0.005	0.012 ± 0.003		0.0007	
7	Ketanserine (KET)	1.7 ± 0.2	0.54 ± 0.07		0.170	
9	Histamine	4500 ± 600	143 ± 12	436 ± 36	-	
10	Phenylethylamine	34 ± 5	3.7 ± 0.5			
11	Amphetamine (+)	47 ± 6	2.1 ± 0.2			
12	Amphetamine (−)	259 ± 33	10 ± 1.7			
13	MDMA (+/−)	19 ± 3	6.9 ± 1.0			
14	Fenfluramine	3.1 ± 0.4	5.1 ± 0.5			
15	MPP+	69 ± 10	8.9 ± 1.4		9.7	1.5

[a] Determined using digitonin permiabilized CV-1 cells expressing c DNA of hVMAT1 and hVMAT2 in the presence of ATP. The apparent K_m and V_{max} parameters determined with [^{3}H]5HT for VMAT1 and VMAT2 were 1.3 μM and 0.8 μM and 37 and 43 pmoles/min.450,000 cells, respectively. Inhibition of [3H]5HT uptake (90 nM) in the presence of various substrates were determined and Ki values were estimated by nonlinear regression analysis[20].
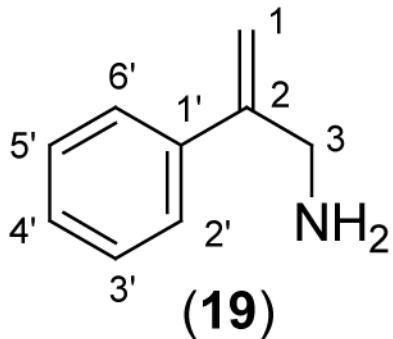
[b] Determined using the membranes prepared from the COS cells transfected with hCGVMAT uptake in the presence of ATP. The apparent K_m determined for [3H]5HT uptake was 0.3 μM. Inhibition of [^{3}H]5HT uptake in the presence of various substrates were determined and K_i values were estimated by nonlinear regression analysis[41].

[c] Determined using homogenized COS cells expressing c DNA of bVMAT2 in the presence of ATP. The apparent K_m and V_{max} parameters were determined for [^{3}H] norepinephrine were 1.9 μM and 32 pmoles/min.mg. The affinities of the substrates with respect to [^{3}H] norepinephrine (IC$_{50}$ values) were estimated by competitive experiments[42].

[d] Taken from the ref. [42].

Table III

Inhibition Kinetic Parameters of APP Derivatives for bVMAT[a]

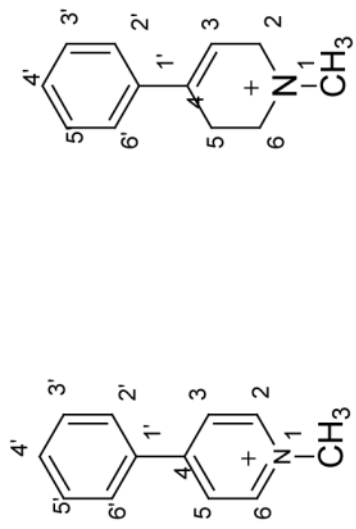|	APP Derivative	$K_i (\mu M)^a$	$K_{m, DA}/K_i{}^d$
19	APP	40.3 ± 5.3	0.57
20	4′-OH APP	15.5 ± 0.9	1.52
21	3′-OH APP	16.7 ± 1.1	1.40
22	4′-OMe APP	102.5 ± 8.1^b	0.33
23	3′-OMe APP	30.2 ± 1.5	0.76
24	4′-F APP	42.3 ± 3.1^b	0.80
25	4′-Cl APP	18.0 ± 0.9^b	1.76
26	4′-Br APP	17.7 ± 2.0	1.79
27	4′-I APP	12.9 ± 2.3	2.96
28	4′-Me APP	55.9 ± 4.4^b	0.59
29	N-Me 4′-OH APP	93.7 ± 11.8	0.39
30	N,N Diethyl 4′OH -APP	202 ± 42^b	0.15
31	N,N,N Trimethyl APP	c	-
32	Phenyl Pyridyl Methyl Ethane	241 ± 84^b	0.12
33	3-Me APP	78.4 ± 24.6^b	0.41
34	N,N Diethyl 3-Me 4′-OH APP	207 ± 37^b	0.15
35	4′-OH 1-Br(E) APP	50.0 ± 6.1^b	0.46
36	4′-OMe 1-Br (E) APP	c	
37	2′-Me, 4′OH APP	c	

[a]Determined with resealed granule ghosts using DA as the substrate in the presence of 10 mM ATP, at pH 7.2.

[b]Estimated from a set of single inhibitor concentration data set;

[c]Relatively weak inhibition was observed.

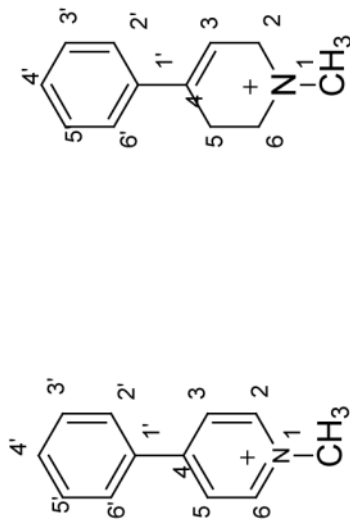[d]Included for comparison purposes (for further details *see* ref. [53]).

Table IV

Uptake and Inhibition Kinetic Parameters of MPTP and MPP⁺ Derivatives for Bovine Chromaffin Granule VMAT.[a]

MPP⁺ (**15**)   MPTP (**51**)

Inhibitor/Substrate	K_i (μM)[a]	K_m (μM)[b]	V_{max} (nmols/mg.min)[b]	$K_{m,DA}/K_i$[c]
		MPP⁺ Derivatives		
15 MPP⁺I⁻	92 ± 14	73 ± 11	1.4 ± 0.1	0.3
38 2′-MeMPP⁺I⁻	95 ± 10			0.3
39 3′-OHMPP⁺I⁻	2.4 ± 0.1	8.4 ± 2.1	1.9 ± 0.1	9.7
40 4′-OHMPP⁺I⁻	82 ± 11	107 ± 16	1.6 ± 0.1	0.7
41 4′-OMeMPP⁺I⁻	106 ± 14[d]	135 ± 9	1.6 ± 0.1	0.2
42 3-Me 4′-OHMPP⁺I⁻	65 ± 19[d]			0.8
43 4′-FMPP⁺I⁻	51.3 ± 6.3[d]			1.0
44 4′-ClMPP⁺I⁻	7.6 ± 0.7			5.8
45 3′-ClMPP⁺I⁻	46.3 ± 5.4[d]			1.1
46 4′-CF₃MPP⁺I⁻	33.8 ± 4.2[d]			1.3
47 3′-CF₃MPP⁺I⁻	24.6 ± 3.0[d]			1.8
48 4′-CH₃MPP⁺I⁻	51.8 ± 8.7	41.3 ± 6.6	0.9 ± 0.1	1.0
49 4′-OHN3PP⁺I⁻	338 ± 142			0.1

MPP⁺ (15)

MPTP (51)

Inhibitor/Substrate	K_i (μM)[a]	K_m (μM)[b]	V_{max} (nmols/mg.min)[b]	$K_{m,DA}/K_i$[c]
50 3'-OHN3PP⁺I⁻	36.6 ± 4.3[d]			1.2
		MPTP Derivatives		
51 MPTPHCl	52.5 ± 6.3	409 ± 88	1.7 ± 0.3	0.5
52 2'-MeMPTPHCl	38.4 ± 5.2			0.7
53 2'-NH₂MPTPHCl	193 ± 39[d]			0.1
54 3'-OHMPTP HCl	25.8 ± 3.1[d]			1.7
55 4'-OHMPTP HCl)	134 ± 24[d]			0.3
56 3'-ClMPTP HCl	27.7 ± 3.4			1.6
57 4'-F MPTP HCl	49.7 ± 6.3[d]			0.9
58 MPDP⁺ClO4⁻	53.0 ± 13.6[d]			0.7

[a]Determined with resealed granule ghosts using DA as the substrate in the presence of 10 mM ATP, at pH 7.2.

[b]Determined from initial rate uptake data under the same conditions;

[c]Included for comparison purposes.

[d]Estimated from a set of single inhibitor concentration data set (for further details *see* ref. [55]).

Table V

Inhibition Kinetic Parameters of MPP[+]-APP Conjugates for Bovine Chromaffin Granule VMAT.[a]

(59) R = H; (64) R = H, 4'-OMe;
(65) R = I; 3'-OH; (66) R = Br; 4'-OH;
(67) R = Ph

Inhibitor	K_i (μM)[a]	$K_{m,DA}/K_{i,I}$[b]	Inhibitor	K_i (μM)[a]	$K_{m,DA}/K_{i,I}$[b]
59	38.4 ± 4.2	0.9	64	2.8 ± 0.1	8.7
60	53.0 ± 13.6	0.7	65	0.4 ± 0.1	55
61	16.4 ± 2.7	1.8	66	0.5 ± 0.1	41.5
62	13.4 ± 1.7	2.7	67	4.5 ± 0.5	11.3
63	1.4 ± 0.2	24.1			

[a]Determined with resealed granule ghosts using non-radioactive substrates with HPLC-EC quantification of catecholamine uptake in the presence of 10 mM ATP, at pH 7.2.

[b]Included for comparison purposes (for further details *see* Table IV foot notes and ref. [55]).

Table VI

VMAT Inhibition Kinetic Parameters of Lobeline Derivatives

Cpd.	K_i (µM)[a]	Cpd.	K_i (µM)	Cpd.	K_i(µM)
68	2.8 ± 0.6	71	19.4 ± 1.3	74	5.3 ± 0.5
69	9.9 ± 2.2	72	1.0 ± 0.2	75	0.57 ± 0.07
70	7.1 ± 2.4	73	6.5 ± 1.7	76	0.6 ± 0.2

[a]K_i parameters were determined by measuring the inhibition of [^{3}H]DTBZOH binding to the rat striatal synaptic vesicles[59].

[b]Taken from ref. 168

Table VII

VMAT Inhibition Kinetic Parameters of Tetrabenazine and its Derivatives

Cpd.	Source of VMAT	VMAT Affinity K_d or K_i (nM)	Refs.
5	Chromafin granule memb.	1.3^a	34
78	Rat brain homog.	6^b	82
79	Rat brain homog.	20^b	82
80	Rat brain homog.	3.9^c	77, 78
81	Rat brain homog.	2.6^d	85
82	Rat brain homog.	12^d	85
83	Chromaffin granule memb.	6^c	36
84	Chromaffin granule memb.	110^b	36
85	Rat brain homog.	28^b	145
86	Rat brain homog.	~ 25–30	83
87(+)	Rat brain homog.	0.22^a	81, 84
88(±)	Mouse striatal homog.	0.76^a	86
89(±)	Mouse striatal homog.	0.56^a	86
89(+)	Mouse striatal homog.	0.1±0.01	88
90(+)	Rat striatal homog.	0.08	91

[a] K_d.

[b] K_i for [^{3}H]DTBZOH binding.

[c] IC_{50} for [^{3}H]DTBZOH binding.

[d] K_i for [^{3}H]MTBZ binding.

Table VIII

VMAT Inhibition Kinetic Parameters of Ketanserin Derivatives

Cpd.	K_i or K_d (nM)		Cpd.	K_i or K_d (nM)	
	Chromaffin Gran. Memb.	Rat cortex		Chromaffin Gran. Memb.	Rat cortex
7	$45.3 \pm 2.4(30°)^a$ $6.3 \pm 0.4 (0°)^a$	1.3^d	**94**	40^b	1.4^d
91	23^b	-	**95**	814^b	0.9^d
92	14^b	0.7^d	**96**	950^b	-
93	350^b	890^d	**97**	950^b	2.3^d
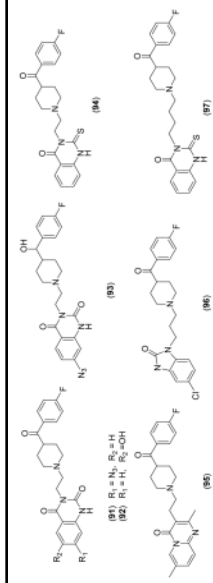
$^a K_d$ determined using [^{3}H] ketanserin at 0° and 30 °C [36].

$^b K_i$ for [^{3}H]DTBZOH binding at 22° C[93];

$^c K_d$ determined using [^{3}H] ketanserin at 0°C [93].

$^d K_d$ determined using [^{3}H] ketanserin at 37° C[36].